

Spectroscopic Studies of Diatomic Indium Halides

S. K. Mishra, Raj K. S. Yadav, and V. B. Singh^{a)}

Department of Physics, Udai Pratap Autonomous College, Varanasi 221002, India

S. B. Rai

Department of Physics, Banaras Hindu University, Varanasi 221005, India

(Received 1 November 2002; revised manuscript received 7 March 2003; accepted 3 June 2003; published online 2 April 2004)

A critical review of the available spectroscopic information about diatomic indium halides has been performed. The literature was surveyed till early 2002 and the data on the molecular constants for the ground state, as well as excited states of these molecules has been presented. A brief discussion on the dissociation energies, ionization potentials, and the nature of the bonding in the ground state is given. The energy level diagram and Rydberg–Klein–Rees potential curves for the different electronic states of these molecules are also presented. Mechanism of laser emission/fluorescence due to atomic indium in the ultraviolet photodissociation of indium monohalides has also been discussed. © 2004 American Institute of Physics. [DOI: 10.1063/1.1595652]

Key words: diatomic indium halides; dissociation energy; ionization potential, molecular spectroscopic constants, photodissociation lasers.

Contents

1. Introduction.	454
2. Ground State.	454
2.1. Nature of Bonding in the Ground State.	454
2.2. Photoelectron Spectra.	456
2.3. Ground State Dissociation Energy.	457
2.4. Ionic Character of the Bond in Indium Monohalides.	458
3. Microwave Spectroscopic Studies.	458
4. Properties of Low-Lying Excited States.	462
4.1. The $A-X$ and $B-X$ Systems.	464
4.1.1. InF.	464
4.1.2. InCl.	464
4.1.3. InBr.	465
4.1.4. InI.	465
4.2. The $C-X$ system.	465
4.2.1. InF.	466
4.2.2. InCl.	466
4.2.3. InBr.	467
4.2.4. InI.	467
4.3. The $D-X$ System.	467
5. Rydberg States.	467
5.1. InCl.	467
5.2. InF, InBr, and InI.	468
6. Laser Emission by Photodissociation of Indium Monohalides.	468
7. Conclusion.	469
8. Acknowledgments.	469
9. References.	469

List of Tables

1. Adiabatic and vertical ionization potentials (eV) of InF, InCl, InBr, and InI.	456
2. Ground state dissociation energy (eV) of indium monohalides using different methods.	458
3. RKR potential energy curve for (A) the ground state ($X^1\Sigma^+$) and (B) the $A^3\Pi_0$ and $B^3\Pi_1$ states of indium halides.	459
4. Ionic character for indium monohalides.	462
5. Molecular constants of the $X^1\Sigma^+$, $A^3\Pi_0$, $B^3\Pi_1$, and $C^1\Pi$ states of indium monohalides.	463
6. Nuclear quadrupole coupling constants and spin rotation constant of indium monohalides.	463
7. Summary of the spectroscopic information for the Rydberg states of InCl.	467

List of Figures

1. Energy level diagram (not to scale) for the low-lying excited states of indium monohalides.	455
2. Variation of vibrational constant (ω_e) in ground state with total number of electrons.	456
3. Variation of experimental and extrapolated D_e values in indium monohalides.	458
4. Nuclear quadrupole coupling constant (eq_0Q) of the metal atom vs internuclear distance (r_e) in IIIA/halogen diatomic molecules.	464
5. Potential energy curve for the $X^1\Sigma^+$ and $C^1\Pi$ states of the InBr molecule.	467
6. Energy level diagram of indium halides and neutral indium relevant to indium photodissociation laser.	468

^{a)}Author to whom correspondence should be addressed; electronic mail: vipin_vns@sify.com
© 2004 American Institute of Physics.

1. Introduction

Indium halides are an excellent system to work with both from the basic and applications point of view. Their diatomic halides are transient, short lived molecular species, normally appear in the gas phase and have many attractive physical and chemical properties, such as high volatility at reasonably low temperatures, fast recombination rates and fairly low dissociation energies. For the last two decades, interest in the study of IIIA group metal halides has been rather high, in part due to their potential applications as atomic photodissociation^{1–5} and nonresonant anti-Stokes Raman lasers.⁶ These are also used in lighting industry^{7,8} and in the manufacturing of semiconductor devices (including integrated circuits).⁹ Indium iodide is an important additive to mercury discharge lamps.¹⁰ These potential applications have emphasized the need for basic data on radiative and structural properties of these molecules, and diatomic indium halides have been subject to rather extensive spectroscopic investigation.

The electronic spectrum of indium halides (InF, InCl, InBr, and InI) consists mainly of three band systems in the visible-ultraviolet region of the spectrum. These systems are attributed to $A^3\Pi_0(0^+) - X^1\Sigma^+(0^+)$, $B^3\Pi_1(1) - X^1\Sigma^+(0^+)$ and $C^1\Pi(1) - X^1\Sigma^+(0^+)$ transitions (see Fig. 1). These spectra show some interesting features: the formation of head of heads, the reversal of shading, and the appearance of extra heads in a band. The electronic spectra of these indium halides (exclusive of InF) was first observed by Petrikaln and Hochberg¹¹ and then by Wehrli and Miescher.¹² The electronic spectrum of InF was first studied by Welti and Barrow¹³ and by Barrow *et al.*^{14,15} No spectroscopic data are available on the fifth monohalide of indium, namely indium astatide. These early studies on these molecules have been further augmented by work from several groups of researchers.^{16–24} Extensive vibrational and rotational analyses on these molecules have been carried out after 1985 by Borkowska-Burnecka and Zyrnicki,^{25,26} Perumalsamy *et al.*,^{27,28} Vempati and Jones,^{29–35} Singh *et al.*,^{36–39} Wolf and Tiemann,^{40,41} Davis and Pecyner,⁴² many others,^{43–45} and most recently by Saksena and Deo.^{46,47} Recently Li *et al.*^{48,49} have reported on laser fluorescence spectra of InCl. More recently, theoretical studies on these molecules have been carried out.^{50–54} Microwave spectral studies on these indium halides have been performed by a number of researchers.^{55–69} Two photon induced dissociation of InCl and InBr have been shown to lead to excited In atoms which decay to the ground state yielding laser emission.⁷⁰ A similar lasing transition has been observed in the atoms obtained through one photon dissociation of InI.¹

In the present paper, we summarize the available spectroscopic information for the diatomic indium halides and indicate with a view to emphasize the existing inconsistencies in data and gaps in our knowledge. Any information available on the isotopic molecules is also included. A brief discussion (including data) on the dissociation energies, percentage of ionic character and ionization potential of these molecules

are given. The Rydberg–Klein–Rees (RKR) potential curves for ground and the low-lying excited states are computed. The review is arranged in the following manner. The second section (consisting of four subsections) covers the ground state properties and includes: Sec. 2.1—discussion of the results of the quantum mechanical calculations of electronic structures, Sec. 2.2—the photoelectron spectra, Sec. 2.3—the dissociation energy, and Sec. 2.4—the calculated percentage ionic characters.

In Sec. 3 the results obtained from the studies of the microwave spectra are summarized. The results for the low-lying excited electronic states are discussed in Sec. 4, whereas Sec. 5 provides a summary of the available information about the Rydberg states and states of corresponding molecular ions. Section 6 deals with the studies related to the photodissociation of these diatomic metal halides and consequent laser emission.

2. Ground State

2.1. Nature of Bonding in the Ground State

The indium monohalides are diatomic molecules with an even number of electrons. These monohalides (in fact all IIIA group monohalides) have a certain apparent simplicity as there is one p electron outside a closed s subshell in the indium (metallic) atom and one hole in the np shell of the halogen atom. In a qualitative manner the bonding will thus be described mainly in terms of $5s$ and $5p$ atomic orbitals of indium and the ns and np orbitals of the halogens ($n = 2, 3, 4, 5$ for F, Cl, Br, and I, respectively). The most important contribution is in the interaction between the In($5s^2$) $5p$ and the halogen np^5 electrons. The six electrons are to be distributed over a strongly bonding σ orbital, a doubly degenerate π orbital with dominant halogen lone-pair character, and another σ type orbital, which may have a small antibonding character. The ground state electronic configuration of these diatomic indium halides can be written as $\dots(y\sigma)^2(w\pi)^4(x\sigma)^2$ leading to the $^1\Sigma^+$ (for Case a or Case b types of coupling and 0^+ for Case c type of coupling) state.

The ground state electronic configuration of the constituent atoms, namely indium (In) and halogens (X), where $X = \text{F, Cl, Br, I}$, both generate a 2P term, which is regular for In and inverted for X. These atomic states can lead to $^1\Sigma^+$, $^3\Pi_0$, $^3\Pi_1$, $^1\Pi$, \dots molecular states (refer to Fig. 1), of which $^1\Sigma^+$ is the ground state. However, as shown in Sec. 2.3, the ground state of InX may also have a considerable ionic character, so that the above correlation of low-lying molecular states with the atomic dissociation products is not straightforward. On the basis of detailed *ab initio* and semiempirical (extended Huckel and complete neglect of differential overlap) quantum chemical calculations for IIIA group monohalides molecules,^{71–76} the following conclusions about the nature and bonding character of the outermost molecular orbitals in the InX molecules are obtained:

- (i) The outermost σ orbital is mainly localized on In and

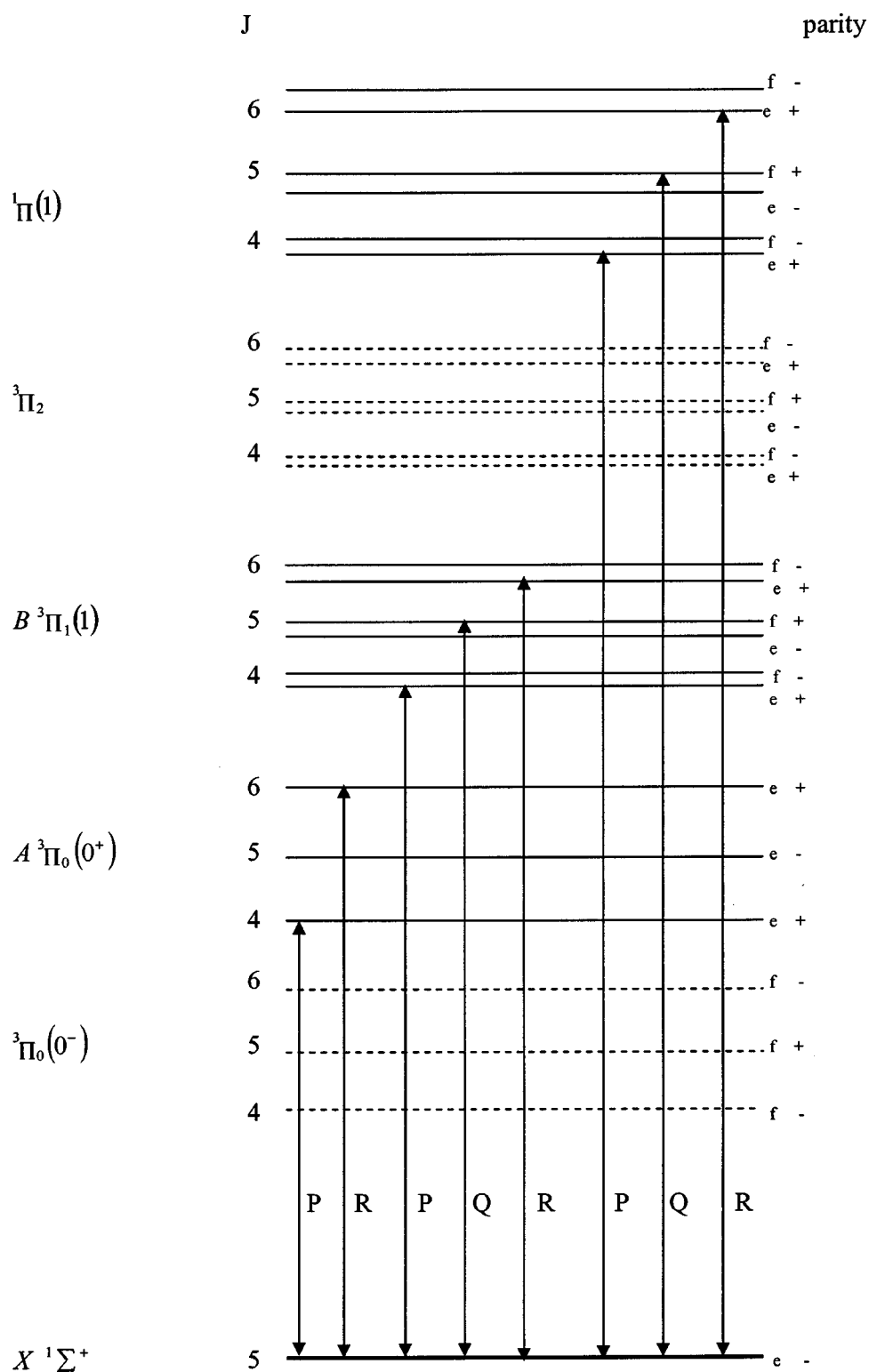


FIG. 1. Energy level diagram (not to scale) for the low-lying excited states of indium monohalides.

is mostly $5s$ in character. The relative contribution of the ns metal orbital in the outermost σ molecular orbital gradually decreases as we go from the fluoride to the iodide.

- (ii) The π orbital is predominantly the $np\pi$ orbital of the halogen though here also as we go from InF to InI contribution of the $np\pi$ orbital of In atom increases.

- (iii) The next inner molecular orbital is another σ orbital which has a behavior complementary to that of the outer σ orbital, i.e., it is mostly a np orbital centered on the halogen atom, with only a small contribution from the ns orbital of the metal.

To better indicate the similarity in energy levels and spec-

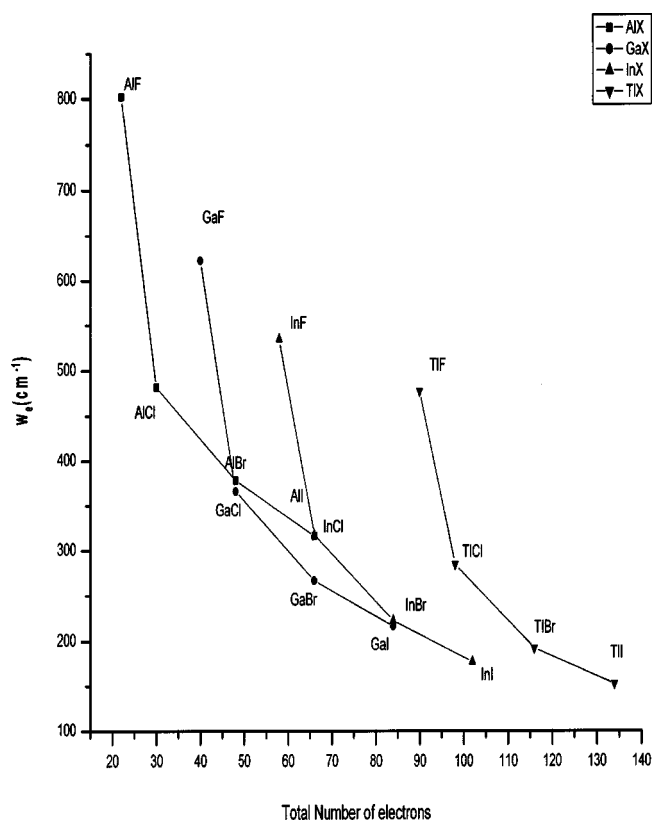


FIG. 2. Variation of vibrational constant (ω_e) in ground state with total number of electrons.

troscopic properties with some other IIIA group monohalides (gallium halides, thallium halides, and aluminum halides), Fig. 2 shows the value of ω_e for the ground state of all these molecules against the total number of electrons in the molecule.^{77,78}

2.2. Photoelectron Spectra

Berkowitz⁷³ and Berkowitz and Dehmer^{74,75} carried out an interesting series of investigations on the photoelectron spectroscopy of some IIIA group monohalide vapors. The photoelectron spectrum has been excited by the He (i) resonance radiation and therefore only ionizations below ~ 20 eV have been observed. The photoelectron spectra of InF was studied by Egdell *et al.*⁷⁶

In general, six diatomic thallium and indium halides (TlCl, TlBr, TlI, InCl, InBr, and InI), studied by Berkowitz⁷³ and Berkowitz and Dehmer,⁷⁴ show three peaks in the photoelectron spectra. The peaks are easily interpreted to involve ionization from the three outermost molecular orbitals leading to the formation of molecular ions in three different low-lying electronic states. In InCl and InBr the first peak is sharp [full width half maximum (FWHM) ~ 0.1 eV] while the second peak is broad (FWHM ~ 0.8 eV). The third peak is again relatively broad. In the case of the iodide the first peak is also relatively broad. It has an area almost twice that of the second peak. The third peak is again broad. The measured ionization potentials for InCl, InBr, and InI adopted from the above references are given in Table 1. The vertical ionization potential refers to the ionization in accordance with the Franck–Condon principle and usually involves a vibrationally excited ionic state. The adiabatic value corresponds to the minima of the corresponding ionic states.

The first peak in the photoelectron spectrum can be attributed to the removal of an electron from the outermost σ orbital (concentrated mainly on the metal atom) leading to the formation of a molecular ion in the $^2\Sigma^+$ state, while the second peak is to be attributed to ionization of an electron from a halogen $p\pi$ orbital, leading to the formation of a $^2\Pi$ state. The third peak corresponds to removal of an electron from a molecular orbital which is complementary to the outermost σ orbital and leads to the formation of another $^2\Sigma^+$ state of the ion.

Grabandt *et al.*⁷⁹ have reported the observation of three peaks in the He (i) photoelectron spectrum of InF. In addition another weak band at the lower energy side is reported. The first peak lying between 10 and 10.5 eV shows a structure with a vibrational spacing of ~ 525 cm⁻¹, which is quite close to ω_e of the InF ground state. The second peak in the photoelectron spectrum lies between 11.5 and 13.2 eV with somewhat lower intensity while the third peak is in between 13.6 and 14.7 eV. The $^2\Pi$ state of InF⁺ is identified to be repulsive, in agreement with an earlier report by Glenwinkel-Mayer *et al.*⁸⁰ Grabandt *et al.*⁷⁹ noted that neutral InF dissociates into In($^2P_{1/2}$) and F(2P) while InF⁺ dissociates into In⁺(1S_0) and F(2P). The dissociation energies for several InF⁺ states are also reported. Table 1 (adapted from the above references) gives the measured ionization potentials

TABLE 1. Adiabatic and vertical ionization potentials (eV) of InF, InCl, InBr, and InI

State	InF ⁷⁹		InCl ⁷⁴		InBr ⁷⁴		InI ⁷⁴	
	Adiabatic	Vertical	Adiabatic	Vertical	Adiabatic	Vertical	Adiabatic	Vertical
X $^2\Sigma$	10.12	10.19	9.51 9.60 ^a	9.75	9.09	9.41	8.50	8.82
$^2\Pi$	11.51 ^a 11.51 ^b	12.47 ^a 12.47 ^b	10.17	10.85	9.62	10.20	8.78 ^a 9.46 ^b	9.10 ^a 9.78 ^b
$^1\Sigma^+$	13.63	13.93	12.82	13.10	12.38	12.74	11.89	12.21

^aFor $^2\Pi_{3/2}$.

^bFor $^2\Pi_{1/2}$.

(both vertical and adiabatic values are quoted) along with qualitative estimates of the associated half widths.

2.3. Ground State Dissociation Energy

Although the electronic configuration and the molecular states corresponding to the observed transitions have been correctly identified, correlation of the low-lying electronic states to their dissociation products and the calculation of the ground state dissociation energy have presented difficulties and are still in some doubt. A survey of the dissociation energies of the ground and low-lying electronic states of group IIIA monohalides was published more than four decades ago by Barrow.^{81,82} It was found that extrapolation of the observed vibrational levels in the ground state leads to a much lower value for the dissociation energy than the value obtained by thermochemical methods. This fact was taken to be in agreement with the expected ionic character of these molecules. Barrow⁸² had proposed estimates for the best values of the dissociation energies for these molecules and had concluded that in most cases the atoms giving rise to the low-lying molecular electronic states in InX are in states of excitation not higher than $\text{In}^*(^2P_{3/2})$ or $\text{X}^*(^2P_{1/2})$. These excited atomic states are the higher energy components of the ground state 2P states of the two separated atoms.

InF: The value of D_e of InF was reported to be 5.4 eV by Bulmicz *et al.*⁸³ using flame photometry while Murad *et al.*⁸⁴ estimated it as 5.25 eV. Murad *et al.*⁸⁴ have reported the values of D_e for all the IIIA group monofluorides and observed that estimates of the dissociation energies obtained by the Birge–Sponer extrapolation of the vibrational levels in the $^1\Pi$ state are higher than the thermochemical values. This is in contrast to the fact that the Birge–Sponer extrapolation of the ground state vibrational levels leads to a lower estimate of the dissociation energy. Recently, Ozaki *et al.*⁸⁵ estimated the ground state dissociation energy of InF using an extrapolation of the ground state vibrational levels obtained from infrared diode laser spectroscopy.

InCl: Perumalsamy *et al.*²⁸ estimated an upper limit for the dissociation energy of InCl as $\sim 37565 \text{ cm}^{-1}$ ($\sim 4.66 \text{ eV}$) from the observed predissociation in the $C^1\Pi$ state. The RKR curve for this state was constructed (Perumalsamy *et al.*²⁸). These authors suggested that the most probable dissociation products for the $C^1\Pi$ state of InCl are $\text{In}^*(^2P_{3/2}) + \text{Cl}(^2P_{3/2})$ as reported by Barrow.⁸² The predissociation in the $C^1\Pi$ state of InCl has also been investigated by Wolf and Tiemann⁴⁰ in the laser induced spectra of the $C-X$ system. They calculated the (rotationless) potential energy curve of the $C^1\Pi$ state directly from the measured line positions and the predissociation level widths. The potential curve of the $C^1\Pi$ state clearly shows a maximum at $r = 2.74 \text{ \AA}$, where the energy is $\sim 37843 \text{ cm}^{-1}$ above the minimum of the ground state potential curve. Taking the ground state dissociation energy as $D_e \sim 4.44 \text{ eV}$ ($\sim 35500 \text{ cm}^{-1}$), a height of potential maximum of 2342 cm^{-1} above the lowest atomic asymptote results. Wolf and Tiemann⁴⁰ concluded that the reason for this maximum is a strongly avoided crossing of two molecular electronic states

of the same symmetry. One of these states is an ionic state which correlates with $\text{In}^+(^1P_1) + \text{Cl}^-(^1S_0)$ and the other is a covalent repulsive state having the asymptote $\text{In}(^2P_{3/2}) + \text{Cl}(^2P_{3/2})$ or $^2P_{1/2}$. In another report, Wolf and Tiemann⁸⁶ extended these arguments to conclude that bonding in the ground state as well as in the low-lying states of this group of molecule is dominated by the ionic interaction.

InBr: Singh *et al.*³⁹ observed fluctuation bands due to the $C-X$ transition in InBr absorption at different temperatures and estimated the dissociation limit of the $C^1\Pi$ state (after an analysis of these bands). The dissociation limit of the C state was correlated to the dissociation products $\text{In}^*(^2P_{3/2}) + \text{Br}(^2P_{3/2})$ and this yields $D_e \sim 31528 \text{ cm}^{-1}$ ($\sim 3.91 \text{ eV}$) for the ground state of InBr.

InI: Vempati and Jones³³ have presented a brief discussion on the ground state dissociation energy and the nature of the chemical bond in InI by assuming the following two cases:

- (i) If the ground state is considered to be a covalent one, the dissociation products, for the X state are $\text{In}(^2P_{1/2}) + \text{I}(^2P_{3/2})$, for the A state $\text{In}^*(^2P_{3/2}) + \text{I}(^2P_{3/2})$ and for the B state, $\text{In}(^2P_{1/2}) + \text{I}(^2P_{3/2})$.
- (ii) If the ground state is considered to be ionic, the products for the X state are $\text{In}^+ + \text{I}^-$, while for the A and B states these will be $\text{In}(^2P_{1/2}) + \text{I}(^2P_{3/2})$.

These authors obtained various estimates of the ground state dissociation energy of InI assuming correlations with different possible dissociation products and using extrapolated values for the dissociation energies for the upper states and the known atomic excitation energies. The most consistent value for the dissociation energy for the ground state was found to be $\sim 27500 \text{ cm}^{-1}$ ($\sim 3.41 \text{ eV}$), when both the state $A^3\Pi_0$ and $B^3\Pi_1$ are correlated to the same dissociation products as given in case (ii) above. This of course means that the ground state correlates with ionic dissociation products which is rather unusual and is unlikely for a molecule like InI.

Values of D_e for the ground state in these molecules have been listed by Huber and Herzberg²⁴ based on the data prior to 1972. The updated estimates for the dissociation energies of these molecules along with some earlier reported estimates are given in Table 2.

Recently, we have estimated the dissociation energies for InF, InCl, InBr, and InI using the curve fitting method (i.e. comparison of the RKR potential with an H–H potential function).⁸⁷ These values agree quite well with the best values (Table 2). The ground state dissociation energy⁸⁸ has been calculated for all these molecules, using $D_e = \omega_e^2/4\omega_e x_e$ with the most recent values for ω_e and $\omega_e x_e$ and compared with the experimental values for D_e (Fig. 3). A large discrepancy is seen between this extrapolated value and the experimental value for InF, but for InI the extrapolated value is almost coincident with the experimental value. This indicates an increasing ionic character in the ground state towards the lighter molecules (InF) in this group, and again shows that ascribing a large ionic character to the ground state of InI is not proper.

TABLE 2. Ground state dissociation energy (eV) of indium monohalides using different methods

Molecule	Thermo-chemical value ⁸²	¹ Π		Best values suggested by Barrow ⁸²	Best values suggested by Huber and Herzberg ²⁴	Our value by curve fitting method ³⁹
		Extrapolated ^{82,85,39,33}	Predissociation ^{28,37}			
InF	5.25±0.15	5.28	...	5.46	5.25	5.25
InCl	4.44	4.43	4.66	4.44	4.44	4.44
InBr	3.99	3.91	3.71	3.99	3.99	3.99
InI	3.43	3.41	...	3.43	3.43	3.43

The RKR have been computed,⁸⁷ using most recent molecular constants, for the ground states and the low-lying excited states (*A* and *B*) for all the four indium monohalides [Tables 3(A and B)].

2.4. Ionic Character of the Bond in Indium Monohalides

Classical chemical valency theory classifies molecular bonding into separate classes including ionic, covalent, and metallic. The ionic bonding is supposed to involve a transfer of an electron from an electropositive (usually metal) atom to an electronegative (usually halogen) atom while in a covalent bond no transfer of electronic charge takes place. A pure ionically bonded molecule would involve a structure of the type M^+X^- so that it has a dipole moment of magnitude eR_e (R_e being the equilibrium bond length and e the electronic charge). Of course no naturally occurring molecule is purely ionic and we have to define a partial ionic character to denote departure from covalency. There are several empirical expressions given in the literature^{89–92} to calculate the percentage ionic character of a bond. The calculated values for the partial ionic character in indium monohalides using different expressions are given in Table 4. A comparison⁹³ of

the Hellman⁹⁴ and Rittner⁹⁵ curves for the ground state of these molecules with their RKR curves is given which shows an interesting behavior. The ionic curve has an asymptote which is obviously much higher in energy than the asymptote corresponding to dissociation into normal atoms. It is therefore unusual that the ionic curve is much above the actual experimental curve and the two curves may meet or cross only at large internuclear separations. We have also observed a similar trend. This result indicates that the ionic forces make a larger contribution to the bonding in the ground state for indium halides.

3. Microwave Spectroscopic Studies

Investigation of microwave spectra has provided useful information on gas phase molecular structure and molecular interactions. The microwave spectra of indium halides were first studied by Barrett and Mandel.^{55,56} Later on high resolution studies on individual molecules of this group have been reported by different workers.^{57–69} These studies yield reliable values for the rotational constants of the molecule in the ground state. Further analysis yields data on the quadrupole coupling constants which permits a crucial test of the electronic wave function—since the charge densities (rather their gradients) at the nuclear sites along with the quadrupole moment of the nucleus in question are measured.

The millimeter wave rotational spectra of the four isotopic species of InCl and InBr have been studied in the 250–350 GHz frequency region by Hoeft and Nair.^{66,67} They reported improved and extended sets of Dunham parameters and vibrational constants for these molecular species. In InCl a comparison of the most precisely determined Dunham parameter Y_{01} for the isotopic pairs of In³⁵Cl and In³⁷Cl shows deviation from the usual mass relations between the constants for isotopic species, indicating a violation of the Born–Oppenheimer approximation. Hoeft and Nair⁶⁸ also studied the millimeter wave rotational spectra of the two isotopic species of InF in the same spectral region and reported improved and extended sets of Dunham parameters for this molecule. The comparison of the results for the two isotopic species of InF again indicates a deviation from the Born–Oppenheimer approximation. The high resolution ro-

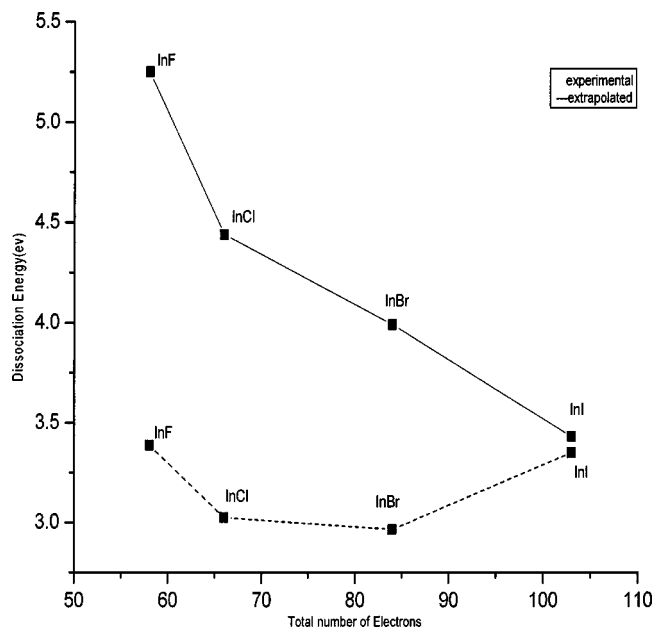


FIG. 3. Variation of experimental and extrapolated D_e values in indium monohalides.

TABLE 3. RKR potential energy curve for (A) the ground state ($X^1\Sigma^+$) and (B) the $A^3\Pi_0$ and $B^3\Pi_1$ states of indium halides

v	G_v	B_v	r_{\min}	r_{\max}
(A)				
$^{115}\text{In}^{19}\text{F}$				
0	266.847	0.261 20	1.927 14	2.051 77
1	796.639	0.259 34	1.887 83	2.104 54
2	1321.269	0.257 48	1.862 49	2.143 41
3	1840.788	0.255 63	1.842 89	2.176 62
4	2355.244	0.253 79	1.826 62	2.206 58
5	2864.687	0.251 96	1.812 59	2.234 37
6	3569.167	0.250 14	1.800 20	2.260 59
7	3868.734	0.248 33	1.789 07	2.285 64
8	4363.437	0.246 53	1.778 96	2.309 75
9	4853.326	0.244 74	1.769 67	2.333 10
10	5338.450	0.242 96	1.761 08	2.355 84
11	5818.858	0.241 19	1.753 08	2.378 06
12	6294.603	0.239 43	1.475 60	2.399 84
$^{115}\text{In}^{35}\text{Cl}$				
0	158.436	0.108 724	2.341 713	2.467 793
1	473.762	0.108 206	2.300 757	2.519 713
2	787.025	0.107 689	2.274 028	2.557 469
3	1098.224	0.107 172	2.253 147	2.589 442
4	1407.361	0.106 654	2.235 684	2.618 063
5	1714.434	0.106 137	2.220 527	2.644 443
6	2019.443	0.105 620	2.207 060	2.669 199
7	2322.390	0.105 102	2.194 899	2.692 717
8	2623.273	0.104 585	2.183 784	2.715 257
9	2922.094	0.104 0678	2.173 5322	2.737 0049
10	3218.851	0.103 5505	2.164 0056	2.758 0962
11	3513.544	0.103 0331	2.155 1008	2.778 6368
12	3806.175	0.102 5157	2.146 7358	2.798 7095
13	4096.742	0.101 9984	2.138 8452	2.818 3806
14	4385.247	0.101 4810	2.131 3753	2.837 7047
15	4671.688	0.100 9636	2.124 2819	2.856 7272
16	4956.065	0.100 4462	2.117 5276	2.875 4862
$^{115}\text{In}^{79}\text{Br}$				
0	111.3351	0.055 576 30	2.489 2581	2.603 0919
1	333.2255	0.055 385 54	2.451 5993	2.649 1382
2	554.0762	0.055 194 78	2.426 8206	2.682 3391
3	773.8875	0.055 004 02	2.407 3449	2.710 2722
4	992.6591	0.054 813 26	2.390 9722	2.735 1377
5	1210.3910	0.054 622 50	2.376 6973	2.757 9413
6	1427.0830	0.054 431 74	2.363 9608	2.779 2425
7	1642.7360	0.054 240 98	2.352 4137	2.799 3905
8	1857.3490	0.054 050 22	2.341 8212	2.818 6208
9	2070.9230	0.053 859 46	2.332 0162	2.837 1006
10	2283.4570	0.053 668 70	2.322 8748	2.854 9541
11	2494.9510	0.053 477 94	2.314 3024	2.872 2764
12	2705.4060	0.053 287 19	2.306 2245	2.889 1421
13	2914.8220	0.053 096 42	2.298 5815	2.905 6114
14	3123.1970	0.052 905 67	2.291 3246	2.921 7332
15	3330.5330	0.052 714 91	2.284 4136	2.937 5483
$^{115}\text{In}^{127}\text{I}$				
0	88.341 03	0.037 123 77	2.687 7824	2.800 3420
1	264.589 20	0.037 013 30	2.650 3423	2.845 5442
2	440.258 80	0.036 902 84	2.625 6646	2.878 0087
3	615.349 90	0.036 792 37	2.606 2498	2.905 2351
4	789.862 40	0.036 681 91	2.589 9189	2.929 4023
5	963.796 40	0.036 571 44	2.575 6759	2.951 5069
6	1137.152 00	0.036 460 98	2.562 9660	2.972 1034
7	1309.929 00	0.036 350 51	2.551 4432	2.991 5383
8	1482.127 00	0.036 240 05	2.540 8744	3.010 0448
9	1653.747 00	0.036 129 58	2.531 0936	3.027 7890
10	1824.788 00	0.036 019 12	2.521 9778	3.044 8940
11	1995.283 50	0.035 908 65	2.513 4330	3.061 4541

TABLE 3. RKR potential energy curve for (A) the ground state ($X^1\Sigma^+$) and (B) the $A^3\Pi_0$ and $B^3\Pi_1$ states of indium halides—Continued

v	G_v	B_v	r_{\min}	r_{\max}
12	2165.167 60	0.035 798 19	2.505 3851	3.077 5435
13	2334.473 30	0.035 687 72	2.497 7750	3.093 2216
14	2503.200 40	0.035 577 26	2.490 5540	3.108 5370
(B)		A state of $^{115}\text{In}^{19}\text{F}$		
0	286.683	0.272 20	1.888 69	2.008 93
1	854.543	0.270 20	1.850 78	2.060 16
2	1415.063	0.268 20	1.826 31	2.098 09
3	1968.243	0.266 20	1.807 32	2.130 69
4	2514.083	0.264 20	1.791 53	2.160 24
5	3052.583	0.262 20	1.777 87	2.187 80
6	3583.742	0.260 20	1.765 77	2.213 96
7	4107.563	0.258 20	1.754 87	2.239 08
8	4624.042	0.256 20	1.744 91	1.263 41
9	5133.183	0.254 20	1.735 73	2.287 14
10	5634.982	0.252 20	1.727 19	2.310 38
		B state of $^{115}\text{In}^{19}\text{F}$		
0	285.4544	0.272 62	1.887 05	2.007 56
1	852.7031	0.270 62	1.849 25	2.058 66
2	1415.547	0.268 62	1.825 06	2.096 24
3	1974.5560	0.266 62	1.806 52	2.128 27
4	2530.2990	0.264 62	1.791 32	2.157 04
5	3083.3480	0.262 62	1.778 42	2.183 57
6	3634.2720	0.260 62	1.767 26	2.208 44
7	4183.6410	0.258 62	1.757 46	2.231 99
8	4732.0240	0.256 62	1.748 80	2.254 45
9	5279.9930	0.254 62	1.741 11	2.275 98
10	5828.1170	0.252 62	1.734 26	2.296 69
		A state of $^{115}\text{In}^{35}\text{Cl}$		
0	169.550	0.114 8832	2.278 2433	2.400 1378
1	505.830	0.114 2154	2.239 2742	2.451 4040
2	838.350	0.113 5476	2.213 9643	2.489 1170
3	1167.110	0.112 8798	2.194 2383	2.521 3543
4	1492.110	0.112 2120	2.177 7579	2.550 4561
5	1813.350	0.111 5442	2.163 4570	2.577 4910
6	2130.830	0.110 8764	2.150 7433	2.603 0536
7	2445.550	0.110 2086	2.139 2481	2.627 5150
8	2754.510	0.109 5408	2.128 7231	2.651 1260
9	3060.710	0.108 8730	2.118 9921	2.674 0654
10	3363.150	0.108 2052	2.109 9243	2.696 4665
11	3661.830	0.107 5374	2.101 4201	2.718 4320
12	3956.750	0.106 8696	2.093 4006	2.740 0434
13	4247.910	0.106 2018	2.085 8031	2.761 3667
14	4535.310	0.105 5340	2.078 5756	2.782 4566
15	4818.950	0.104 8662	2.071 6756	2.803 3593
16	5098.830	0.104 1984	2.065 0668	2.824 1143
		B state of $^{115}\text{In}^{35}\text{Cl}$		
0	169.0018	0.114 576	2.278 4697	2.400 4094
1	503.7158	0.113 788	2.234 7702	2.447 3478
2	834.0438	0.113 001	2.204 7081	2.480 7184
3	1159.9860	0.112 213	2.180 1856	2.508 6212
4	1481.5420	0.111 425	2.158 8621	2.533 3994
5	1798.7120	0.110 638	2.139 6706	2.556 1223
6	2111.4960	0.109 850	2.122 0191	2.577 3849
7	2419.8940	0.109 063	2.105 5383	2.597 5590
8	2723.9060	0.108 275	2.089 9799	2.616 8960
9	3023.5320	0.107 488	2.075 1673	2.635 5755
10	3318.7720	0.106 750	2.060 9693	2.653 7319
11	3609.6260	0.105 912	2.047 2855	2.671 4691
12	3896.0940	0.105 125	2.034 0367	2.688 8698
13	4178.1760	0.104 337	2.021 1592	2.706 0016
14	4458.8720	0.103 550	2.008 6004	2.722 9208
		A state of $^{115}\text{In}^{79}\text{Br}$		
0	113.7828	0.058 302 45	2.429 3748	2.541 9939
1	339.5558	0.058 026 95	2.392 9195	2.588 8753
2	562.9387	0.057 751 45	2.369 0934	2.623 2070

TABLE 3. RKR potential energy curve for (A) the ground state ($X^1\Sigma^+$) and (B) the $A^3\Pi_0$ and $B^3\Pi_1$ states of indium halides—Continued

v	G_v	B_v	r_{\min}	r_{\max}
3	783.9318	0.057 475 95	2.350 4295	2.652 4574
4	1002.5350	0.057 200 45	2.334 7653	2.678 7907
5	1218.7480	0.056 924 95	2.321 1146	2.703 1946
6	1432.5710	0.056 649 45	2.308 9296	2.726 2187
7	1644.0040	0.056 373 95	2.297 8689	2.748 2059
8	1853.0470	0.056 098 45	2.287 7029	2.769 3877
9	2059.7000	0.055 822 95	2.278 2683	2.789 9291
10	2263.9630	0.055 547 45	2.269 4443	2.809 9529
11	2465.8360	0.055 271 95	2.261 1382	2.829 5537
12	2665.3190	0.054 996 45	2.253 2774	2.848 8062
13	2862.4120	0.054 720 95	2.245 8034	2.867 7709
<i>B</i> state of $^{115}\text{In}^{79}\text{Br}$				
0	111.8457	0.058 145 65	2.432 1830	2.545 7798
1	333.6277	0.057 853 55	2.395 6041	2.593 3364
2	552.8638	0.057 561 45	2.371 7463	2.628 2613
3	769.5538	0.057 269 35	2.353 0829	2.658 0831
4	983.6978	0.056 977 25	2.337 4348	2.684 9827
5	1195.2960	0.056 685 15	2.323 8083	2.709 9557
6	1404.3480	0.056 393 05	2.311 6516	2.733 5560
7	1610.8540	0.056 100 95	2.300 6210	2.756 1295
8	1814.8140	0.055 808 85	2.290 4850	2.777 9096
9	2016.2280	0.055 516 75	2.281 0792	2.799 0631
10	2215.0960	0.055 224 65	2.272 2819	2.819 7141
11	2411.4180	0.054 932 55	2.263 9996	2.839 9584
12	2605.1940	0.054 640 45	2.256 1591	2.859 8718
<i>A</i> state of $^{115}\text{In}^{127}\text{I}$				
0	78.584 26	0.038 254 49	2.642 9986	2.762 3806
1	233.848 80	0.038 037 46	2.605 0251	2.813 2898
2	386.574 60	0.037 820 44	2.580 3169	2.851 0668
3	536.761 70	0.037 603 41	2.560 9868	2.883 6028
4	684.410 00	0.037 386 38	2.544 7551	2.913 1815
5	829.519 80	0.037 169 36	2.530 5830	2.940 8462
6	972.090 80	0.036 952 33	2.517 8935	2.967 1782
7	1112.123 00	0.036 735 30	2.506 3271	2.992 5419
8	1249.617 00	0.036 518 28	2.495 6412	3.017 1849
9	1384.572 00	0.036 301 25	2.485 6631	3.041 2853
10	1516.988 00	0.036 084 23	2.476 2641	3.064 9775
11	1646.776 20	0.035 867 20	2.467 3451	3.088 3665
12	1774.115 00	0.035 650 18	2.458 8276	3.111 5372
<i>B</i> state of $^{115}\text{In}^{127}\text{I}$				
0	72.660 39	0.037 713 88	2.659 5026	2.783 6864
1	214.673 80	0.037 425 65	2.620 9798	2.839 0778
2	352.292 60	0.037 137 41	2.595 9179	2.881 2878
3	485.503 10	0.036 849 18	2.576 1698	2.918 4797
4	614.309 80	0.036 560 94	2.559 3845	2.953 0227
5	738.712 80	0.036 272 71	2.544 4865	2.986 0123
6	858.712 00	0.035 984 47	2.530 8721	3.018 0746
7	974.307 60	0.035 696 24	2.518 1580	3.049 6182
8	1085.4990	0.035 408 00	2.506 0777	3.080 9377
9	1192.2870	0.035 119 77	2.494 4331	3.112 2636
10	1294.6720	0.034 831 53	2.483 0675	3.143 7892

TABLE 4. Ionic character for indium monohalides

Molecules	$(X_B + X_A)^a$	$(X_B - X_A)^a$	Percentage ionic character				From the relation I.C. = μ/er^b
			Hanny <i>et al.</i> ⁸⁹	Pouling ⁹⁰	Wilmhurst ⁹¹	Batsanov <i>et al.</i> ⁹²	
InF	5.7	2.3	55.32	61.41	40.35	65.29	35.66
InCl	4.7	1.3	26.72	26.23	27.66	28.68	32.87
InBr	4.5	1.1	21.84	19.57	24.44	21.49	...
InI	4.2	0.8	15.04	10.88	19.05	12.02	...

^a X_B is the electronegativity of the more electronegative atom B and X_A is that for atom A.

^b μ is the dipole moment, e is the electronic charge, and r is the internuclear distance.

tational spectra of InF, InCl, and InBr have been studied by Hensel *et al.*⁶⁹ using a pulsed jet cavity Fourier transform microwave spectrometer, and precise rotational and nuclear quadrupole coupling constants are reported. These data have permitted the first estimates of the nuclear spin-rotation constants for InCl and InBr. The interpretation of these constants has been carried out in terms of the electronic structures of the molecules. Uehara *et al.*⁹⁶ studied the infrared Fourier transform spectrum of InF and determined the molecular constants for the ground state of this molecule. Most recently, Zou *et al.*⁵³ have determined a new value for the nuclear quadrupole moment for ¹¹⁵In by combining experimental nuclear quadrupole coupling constants with four component coupled-cluster single double triple (CCSD(T)) electric field gradient calculations on indium monohalides. Relativistic effects are shown to be almost as important as electron correlation effects, both contributing about 10% each. However, these two contributions are of opposite sign, and almost cancel each other. Lenthe and Baerends⁵² have presented density functional calculations of the electric field gradients in indium and some other metal halides. The ground state molecular constants obtained from the recent microwave studies are given in Table 5, whereas the recent values of nuclear quadrupole coupling constant and nuclear spin rotation constants are given in Table 6.

Nair and Hoefft⁹⁷ have made some interesting intercomparisons of the available data for diatomic halides of Al, Ga, and In (which in a somewhat modified form is reproduced in Fig. 4). These curves show that the eq_0Q (for $v=0$ level) values for the metal atoms change smoothly with the equilibrium internuclear separation and decrease in going from MF to MI. The curve for Ga and In halides are approximately straight lines whereas the graph for Al halides shows a large departure from this straight line behavior. Since the value of the quadrupole moment of the metal atom may be regarded as remaining essentially constant as we go from the metal fluoride to the metal iodide, this dependence of eq_0Q on the internuclear distance must be a reflection of the variation in q_0 —the electric field gradient at the metal nucleus. If the bonding behavior of the six valence electrons—one contributed by the metal atom and other five by the halogen atom—were similar one would expect a common q_0 for all 12 molecules. That this is not so or in other words the nature of bonding changes considerably in going from the fluoride to the iodide is therefore apparent. One point stands out, Ga and In which contain a filled d shell of electrons give rise to

a near straight line variation as compared to Al where no d electrons are present.

4. Properties of Low-Lying Excited States

The low-lying excited states for most of the indium monohalides arise from the following electron configurations:

$$(y\sigma)^2(\omega\pi)^4(x\sigma) \\ \times (v\pi), \quad {}^3\Pi, \quad {}^1\Pi \quad \text{or} \quad (2,1), \quad (1,0^+,0^-).$$

The excited states ³Π and ¹Π are attributed to the molecular configuration $\pi^4\sigma\pi$, which involve an excitation of an electron from a σ orbital to a π orbital. The ³Π state splits into three almost independent ³Π₀, ³Π₁, and ³Π₂ states due to large spin-orbit coupling. The state with $\Omega=0$, i.e., ³Π₀, splits into two levels 0⁺ and 0[−] when second order effects are included. The A ³Π₀(0⁺) behaves almost like a ¹Σ⁺ state. The states with $\Omega>0$, labeled by B ³Π₁ and ³Π₂, are twofold degenerate, and each rotational level is split into two levels due to the coupling of the electronic angular momentum with the molecular rotation. The singlet state is labeled as the C ¹Π state and lies above the ³Π state. Figure 1 shows the energy level diagram and summarizes the allowed transitions between the ground and low-lying excited states of indium monohalides mainly for InBr and InI. Because of the expected tendency of the molecule to obey Hund's Case C coupling, the A ³Π₀ and B ³Π₁ states would behave primarily as $\Omega=0$ and $\Omega=1$ states. This, in combination with the ground ¹Σ⁺ state, would give rise to rotational structure similar to that found in ¹Σ⁺–¹Σ⁺ and ¹Π–¹Σ⁺ transitions. So in InCl, InBr, InI, and even for InF A, B ³Π– X ¹Σ⁺ transitions are very intense. However, no transitions are allowed between X ¹Σ⁺ and ³Π₀(0[−]) and ³Π₂. The C ¹Π state is stable in InF and InCl, although in the latter case it is a very weakly bound state. So the transition C ¹Π– X ¹Σ⁺ degenerates from consisting of a system of well defined, but converging bands (InCl) to fluctuation bands (InBr) and finally to a continuum (InI). A similar trend is known for Al and Ga monohalides also.

Vempati and Jones³⁴ considered the following configuration to explain lowest excited states of InCl:

$$\dots(z\sigma)^2(y\sigma)^2(\omega\pi)^4(x\sigma)(v\pi): \\ A \quad {}^3\Pi_0, \quad B \quad {}^3\Pi_1, \quad {}^1\Pi, \quad (1)$$

TABLE 5. Molecular constants of the $X^1\Sigma^+$, $A^3\Pi_0$, $B^3\Pi_1$, and $C^1\Pi$ states of indium monohalides^a

Molecules	Electronic state	T_e (cm ⁻¹)	ω_e (cm ⁻¹)	$\omega_e x_e$ (cm ⁻¹)	$\omega_e y_e$ (cm ⁻¹)	B_e (cm ⁻¹)	$\alpha_e \times 10^4$ (cm ⁻¹)	$D_e \times 10^8$ (cm ⁻¹)	$\beta_e \times 10^{10}$ (cm ⁻¹)	r_e (Å)
¹¹⁵ In ¹⁹ F	$X^1\Sigma^+$	0.0	535.001	2.6180	-0.008 27	0.262 14	18.7855	25.2096	2.6330	1.985 400
	$A^3\Pi_0$	30 445.86	575.200	3.6700	...	0.273 20	20.0000	25.0000	...	1.945 000
	$B^3\Pi_1$	31 255.74	572.200	2.6300	-0.095 00	0.273 62	20.0000	25.0000	...	1.944 000
	$C^1\Pi$	42 809.2	463.900	7.3500	-0.500 00	0.267 00	50.0000	36.5000	...	1.967 200
¹¹³ In ¹⁹ F	$X^1\Sigma^+$	0.0	535.950	2.6280	-0.008 40	0.262 80	18.7855	25.3107	2.5666	...
¹¹⁵ In ³⁵ Cl	$X^1\Sigma^+$	0.0	317.389	1.0320	-0.000 51	0.108 98	5.17370	5.161 21	0.2410	2.402 024
	$A^3\Pi_0$	27 778.209	340.040	1.8800	-0.006 58	0.115 22	6.67800	5.266 00	9.6900	2.333 273
	$B^3\Pi_1$	28 563.63	339.100	2.1930	-0.029 02	0.114 97	7.87400	5.900 00	...	2.338 645
	$C^1\Pi$	37 568.116	177.270	12.589	...	0.104 069	36.6540	(14.9500) ⁺	...	2.458 000
¹¹⁵ In ³⁷ Cl	$X^1\Sigma^+$	0.0	310.718	0.9860	...	0.104 469	4.85576	6.621 25	0.2500	2.401 192
	$A^3\Pi_0$	27 778.209	332.923*	1.8020*	-0.006 18*	0.110 445*	6.26743*	4.838 80*	8.7176	...
	$B^3\Pi_1$	28 563.63	332.003*	2.1020*	-0.029 72	0.110 208*	7.39116*	5.421 38
	$C^1\Pi$	37 566.592	310.667	12.068*	...	0.099 758*	34.4003*	(12.7200) ⁺	...	2.473 000
¹¹³ In ³⁵ Cl	$X^1\Sigma^+$	0.0	318.040	1.0358	...	0.109 433	5.205 87	51.8976	0.243 30	2.401 194
¹¹³ In ³⁷ Cl	$X^1\Sigma^+$	0.0	311.336	0.9928	...	0.104 919	4.887 13	47.7280	0.219 00	2.401 192
¹¹⁵ In ⁷⁹ Br	$X^1\Sigma^+$	0.0	222.930	0.5198	-0.003 50	0.055 671	1.907 60	1.364 30	0.060 33	2.543 179
	$A^3\Pi_0$	26 597.85	228.163	1.1950	-0.008 80	0.058 323	2.450 00	1.550 00	...	2.483 092
	$B^3\Pi_1$	27 381.25	224.328	1.2730	-0.016 50	0.058 255	2.790 00	1.580 00	...	2.486 253
	$C^1\Pi$	(34 955) (0- v') band of fluctuation band system ³⁹								
¹¹⁵ In ⁸¹ Br	$X^1\Sigma^+$	0.0	221.370	0.5121	-0.008 80	0.054 856	1.865 89	1.313 96	0.059 70	2.543 180
	$A^3\Pi_0$	26 597.871	226.500	1.1820	-0.008 20	0.057 587	2.727 00	1.522 00*	...	2.483 049
	$B^3\Pi_1$	27 381.257	222.701	1.2600	-0.015 70	0.057 441	2.909 00	1.541 00*	...	2.487 100
	$C^1\Pi$	(34 955) (0- v') band of fluctuation band system ³⁹								
¹¹³ In ⁷⁹ Br	$X^1\Sigma^+$	0.0	223.830	0.5238	...	0.056 073	1.928 27	1.409 60	0.061 57	2.543 179
¹¹³ In ⁸¹ Br	$X^1\Sigma^+$	0.0	222.250	0.5164	...	0.055 258	1.886 39	1.368 26	0.059 37	2.543 181
¹¹⁵ In ¹²⁷ I	$X^1\Sigma^+$	0.0	176.827	0.2893	-0.002 32	0.037 179	1.104 70	1.674 00	1.950 00	2.742 126
	$A^3\Pi_0$	25 050.60	157.803	1.2694	-0.003 59	0.038 042	2.133 00	1.940 00	3.130 00	2.699 479
	$B^3\Pi_1$	25 402.91	146.422	2.2019	-0.000 47	0.037 858	2.882 35	2.350 00	5.450 00	2.717 424
	$C^1\Pi$	Continuous with maximum at 31 400 cm ⁻¹								

^aAn asterisk indicates values obtained from isotopic relation and a plus sign indicates corresponding D_0 values.TABLE 6. Nuclear quadrupole coupling constants and spin rotation constant of indium monohalides^a

Spectroscopic constants	¹¹⁵ In ¹⁹ F (X = ¹⁹ F)	¹¹⁵ In ³⁵ Cl (X = ³⁵ Cl)	¹¹⁵ In ³⁷ Cl (X = ³⁷ Cl)	¹¹⁵ In ⁷⁹ Br (X = ⁷⁹ Br)	¹¹⁵ In ⁸¹ Br (X = ⁸¹ Br)	¹¹⁵ In ¹²⁷ I (X = ¹²⁷ I)
eQq_{In} (MHz)	-723.795 746.80*	-657.8487 742.1000*	-657.8913 ...	-633.5756 742.800*	-633.5731 ...	-607.5 744.0*
eQq_X (MHz)	...	-13.7575 -13.7200*	-10.8399 ...	110.6501 108.600*	92.4367 ...	-386.4 ...
C_{In} (kHz)	17.47	10.454	9.980	6.1680	5.9240	...
C_X (kHz)	18.30	1.710	1.190	5.300	5.3600	...

^aValues obtained from DFT calculations (Refs. 52 and 54) are indicated with an asterisk.

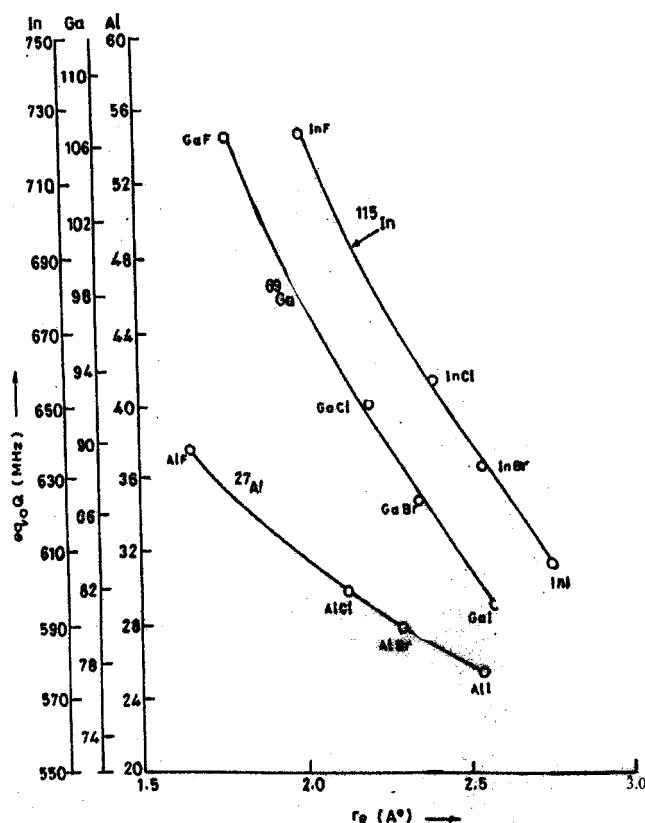


FIG. 4. Nuclear quadrupole coupling constant (eq_0Q) of the metal atom vs internuclear distance (r_e) in IIIA/halogen diatomic molecules.

$$\dots(z\sigma)^2(y\sigma)^2(\omega\pi)^4(x\sigma)(u\sigma):$$

$$^1\Sigma^+, \quad ^3\Sigma^+, \quad (2)$$

$$\dots(z\sigma)^2(y\sigma)^2(\omega\pi)^3(x\sigma)^2(v\pi):$$

$$^1\Sigma^+, \quad ^3\Sigma^+, \quad ^1\Sigma^-, \quad ^3\Delta, \quad ^1\Delta, \quad (3)$$

$$\dots(z\sigma)^2(y\sigma)^2(\omega\pi)^3(x\sigma)^2(u\sigma):$$

$$^3\Pi, \quad ^1\Pi. \quad (4)$$

Vempati and Jones³⁴ concluded that in InCl the $A^3\pi_0$ and $B^3\pi_1$ states arise from configuration (1) while the $C^1\Pi$ state arises from configuration (4) and the C state is predissociated by the $^1\Pi$ state arising from configuration (1). Froslic and Winans¹⁶ also concluded that the state predissociating the $C^1\Pi$ state must be a $^1\Pi$ or a $^1\Delta$ state. However, recent theoretical studies by Zou *et al.*⁵³ have identified the predissociating state as a $^3\Sigma^+$ state.

4.1. The A–X and B–X Systems

The lowest triplet state, $^3\Pi$, whose existence was known in the other (lighter) IIIA group monohalides, has become the most prominent low-lying excited state in the indium halides. These states are fairly stable for this group of molecules.

4.1.1. InF

For InF, the $A^3\Pi_0-X^1\Sigma^+$ and $B^3\Pi_1-X^1\Sigma^+$ transitions give rise to extensive band systems in the spectral region 305–340 nm. Welti and Barrow¹³ carried out the vibrational analysis of these systems of InF in absorption. Barrow *et al.*¹⁴ repeated the vibrational analysis in the emission spectrum and reported that the A, B–X systems of InF are more strongly developed in emission and many more bands are observed. Accurate vibrational constants were determined for the A, B, and X states. Later on Barrow *et al.*¹⁵ carried out rotational analysis of a few bands of both A–X and B–X systems. Molecular constants for the A, B, and X states of InF are given in Table 5.

4.1.2. InCl

In the case of InCl, the strong A–X and B–X systems appear both in absorption and in emission in the region 332–373 nm. A large number of investigations have been carried out on the spectra of InCl. Youngner and Winans¹⁷ reported the first rotational analysis of a few bands of the A–X and B–X systems. Later researchers have concentrated their efforts on improving the accuracy of the measured rotational and vibrational constants. Much of the recent work has been summarized by Borkowska and Zyrmicki,^{25,26} Perumalsamy *et al.*,²⁷ and by Vempati and Jones.³⁴ Recently Li *et al.*^{48,49} reported laser induced fluorescence spectra of InCl molecule in the spectral regions 332–373 and 266.5–287 nm and most recently Saksena and Deo^{46,47} reported a new rotational analysis of the A–X system of InCl from high resolution emission spectrum recorded on Fourier Transform Spectrometer.

Perumalsamy *et al.*²⁷ were able to observe a large number of bands involving higher vibrational levels in the A–X and B–X systems of InCl (up to $v=16$ in the A state, $v=16$ in the X state, and $v=14$ in the B state). They have observed the formation of head of heads in the sequences $\Delta v = +2, +3, +4$ of the A–X system and in the sequences $\Delta v = +2, +3$ of the B–X system. In the 0–0 sequence of the A–X system, (0,0), (1,1), (4,4) and still higher members of the sequence are seen, whereas (2,2) and (3,3) bands are absent. These results are in agreement with the values for the Franck–Condon factors calculated by Ashrafunnisa *et al.*²⁰ These (2,2) and (3,3) bands are also not observed in the laser induced fluorescence spectra of InCl, reported recently by Li *et al.*^{48,49}

Vempati and Jones³⁴ have observed the spectra of InCl at moderately high resolution and carried out an extensive rotational analysis of eleven bands of the A–X system. By extending the analysis of (0,0) band (of the A–X system) to higher rotational levels they have established that rotational perturbations reported earlier reaches its maximum at $J=117$. An additional perturbation in the (1–0) band of A–X system at $J\sim 105$ was also proposed. Improved molecular constants were reported. More recently Saksena and Deo^{46,47} have rotationally analyzed the (1,0), (2,1), (0,0), (0,1), (1,2), (0,2), and (1,3) bands of the A–X system but they have not

been able to locate any rotational perturbations in $v=0$ and 1 levels of the $A\ ^3\Pi_0$ state. This has put the earlier reports of such rotational perturbations in the A state of InCl by Vempati and Jones³⁴ and by others in doubt. Balfour⁹⁸ recently reassigned a system of bands ascribed to InCl by Nampoori and Patel²³ as the $B-X$ system of InCl⁺. This reassignment conveniently removes the difficulty of explaining the unexpected presence of another low-lying excited $^1\Sigma$ state in InCl. The updated values of the molecular constants for the A , B , and X states of InCl are given in Table 5.

4.1.3. InBr

In InBr, strong $A-X$ and $B-X$ systems are also observed both in absorption and emission in the region 354–398 nm. The vibrational analysis of the $A-X$ and $B-X$ systems was first carried out by Pertrikaln and Hochberg¹¹ and Wehrli and Miescher.¹² This was revised and extended by Lakshminarayana and Harnath¹⁸ who photographed the bands of the $A-X$ and $B-X$ systems in emission at better resolution and dispersion. Although the spectra of InBr have been known since 1933, the rotational analysis of only a few bands in the $A-X$ and $B-X$ was reported by Nampoori and Patel²² in 1976. Recently extensive rotational analysis of a large number of bands in these systems has been carried out and more accurate molecular constants for InBr have been reported by Vempati and Jones,^{29,31} Singh *et al.*,^{36–38} and by Borkowska and Zyrnicki.²⁶

Vempati and Jones²⁹ and Borkowska and Zyrnicki²⁶ have recorded the high resolution spectra of InBr only in emission, whereas Singh *et al.*^{36,37} recorded both absorption and emission spectra of InBr at moderately high resolution. A noteworthy feature of the spectrum is that while the individual bands of the $A-X$ and $B-X$ systems are shaded to the violet indicating that $B' > B''$, the structure of the sequences indicate that $\omega' > \omega''$. Apart from the isotope effects, bands with single heads (P heads) and double heads (P and Q) are observed and have been assigned to the $A0^+ - X0^+$ and $B1 - X0^+$ transitions, respectively. Due to bromine isotopic effects most of these band heads are observed to be double. Singh *et al.*³⁶ reported new bands (involving vibrational levels up to $v' = 13$ in the A state, up to $v' = 12$ in the B state, and up to $v'' = 15$ in the X state) including additional sequences with $\Delta v = +5, -5, -6, -7$ in the $A-X$ and with $\Delta v = +4, +5, -6, -7$ in the $B-X$ system. Several of these sequences show the formation of a head of heads and under higher resolution some folding over of the rotational structure is also seen. It is these features which cause the vibrational structure to appear complex and which makes the use of sufficiently high resolution a necessity even for a satisfactory vibrational analysis.

Singh *et al.*³⁶ reported the appearance of bands involving high values of v'' in several sequences in the absorption spectrum of this molecule even though the absorption spectrum was recorded at approximately 600 °C cell temperature. In accordance with Boltzmann distribution law the expected population in $v > 3$ levels of the ground state would be quite small and this population would become almost insignificant

for $v > 6$. It is therefore surprising that bands like (9,10), (10,10), and (9,11) appear in the absorption spectrum. Singh *et al.*³⁶ suggested a step-wise excitation relaxation mechanism for populating the $v = 10, 11$ levels in the ground state.

A natural sample of indium monobromide contains 48.37% $^{115}\text{In}^{79}\text{Br}$ and 47.30% $^{115}\text{In}^{81}\text{Br}$. The consequences are that the rotational lines of these two isotopic molecules would be of similar intensities and lie close together. Rotational analysis of a large number of bands in the $A-X$ and $B-X$ system has been carried out by Vempati and Jones²⁹ and also by Borkowska and Zyrnicki.²⁶ The reported molecular constants are included in Table 5. RKR Potential energy curves for the A , B , and X state and Franck–Condon factor and r centroids for the $A-X$ and $B-X$ system of InBr have been reported by Singh *et al.*³⁸ Franck–Condon factors reflect most of the observed features of the intensity distribution in these systems.

4.1.4. InI

For InI, the $A-X$ and $B-X$ systems are observed in the region 390–440 nm. Wehrli and Miescher¹² for the first time carried out the vibrational analysis of $A-X$ and $B-X$ transition of InI. Recently, Vempati and Jones^{30,32,33} have observed high resolution spectra in emission of InI in order to obtain accurate vibrational and rotational constants for the A and B states of this molecule. They have reported the rotational analysis of almost 21 bands (of the sequences 0–0, 1–0, 0–1, and 0–2) in the $A-X$ system and of ten bands (of the 1–0, 0–0, 0–2 sequences) in the $B-X$ system of InI. In both systems, the reversal of shading and extra heads were observed. The reversal of shading in some sequences of a band system provides a method of rapidly estimating the values for the equilibrium rotational constants of the upper state provided the rotational constants of the lower states are known. Vempati and Jones³⁰ have determined the value of rotational constants for the upper states by using this method and obtained values quite in agreement with those values determined by the more rigorous methods.

Davis and Pecyner⁴² have recorded the high resolution absorption and emission spectra of InI and observed 20 new band heads. They have reported improved vibrational and rotational constants for A and B states of InI.

More recently, Bruchhausen *et al.*¹⁰ have performed a coherent anti-Stokes Raman scattering experiment (RECARS) on InI using a frequency tripled Nd–YAG laser at 355 nm pumping two dye laser systems oscillating near 411 nm. The spectral positions of possible RECARS lines of InI were calculated up to rotational quantum number $J = 280$ and vibrational quantum number $v = 10$. Highly accurate molecular constants were reported. The updated molecular constants for InI are included in Table 5.

4.2. The $C-X$ system

The $C\ ^1\Pi$ state in indium monohalides as well as in all IIIA group monohalides becomes progressively less stable as the mass of the halogen increases. Thus whereas in the

lighter molecule InF, the $C^1\Pi$ state is a fairly stable state and, a transition from this state to the $X^1\Sigma^+$ ground state gives rise to an extensive band system, its stability decreases rapidly in going to heavier molecule. In InCl, $C^1\Pi$ is a weakly bound, rather anharmonic, state (with $\omega_e \sim 177\text{ cm}^{-1}$ and $\omega_e x_e \sim 12\text{ cm}^{-1}$) and shows a predissociation effect. In InBr this state has either a very shallow minimum or is a totally repulsive state, and in InI it is a completely repulsive state.

4.2.1. InF

The $C^1\Pi-X^1\Sigma^+$ system of InF was initially observed in absorption by Welti and Barrow,¹³ and in emission by Barrow *et al.*¹⁴ This system consists of red degraded double headed bands lying between 227.5 and 247.5 nm. The vibrational analysis of these bands has been carried out and vibrational constants were reported.^{13,14} Barrow *et al.*¹⁵ were the first to carry out a rotational analysis of this system and to report the rotational constant for the $C^1\Pi$ state. Further, Nampoori and Patel¹⁹ presented an extensive rotational analysis of a number of bands of the $C-X$ transition in InF. They have observed that the bands form a head in the R branch and degrade towards the longer wavelength side although $B'_v > B''_v$. Two Q heads were also observed. The analysis was carried out for the R and P branches. Due to the small value of $(B'-B'')$, the centrifugal distortion term in the branch equation plays an interesting and important role. The molecular constants for this state are given in Table 5.

4.2.2. InCl

The $C^1\Pi-X^1\Sigma^+$ system of InCl appears in the region 265–283 nm and this was first observed in absorption by Grotian.⁹⁹ The bands in this system are red shaded and are double headed. These bands were correctly identified, initially by Miescher and Wehrli.^{100,12} Miescher and Wehrli^{100,12} observed the absorption spectrum of this system (with three vibrational levels, e.g., $v'=0, 1, 2$ of the excited state) and noted the predissociated nature of the $C^1\Pi$ state. An absorption spectra of the $C-X$ system in an air–acetylene flame was also presented by Haragachi and Fuwa,¹⁰¹ in which they reported seven vibrational levels ($v'=0-6$) of the $C^1\Pi$ state. Recently doubts have been expressed about this observation.¹⁰¹

The rotational analysis of the $C-X$ system of InCl was first reported by Froslic and Winans.¹⁶ However, the ground state constants obtained from this rotational analysis are not in agreement with subsequent microwave values and the rotational analysis was found to be incorrect by many authors. Borkowska and Zyrnicki,²⁵ Perumalsamy *et al.*,²⁸ Wolf and Tiemann,⁴⁰ and Jones and McLean³⁵ have all contributed to work on this system and accurate molecular constants for the $C^1\Pi$ state of InCl are now known (Table 5). Perumalsamy *et al.*²⁸ reported on the diffuse nature of the (3,0) band of the $C-X$ system at low resolution in absorption, though this was not reported by any of the other authors.^{25,35,40} They suggested that predissociation in the $v=0$ and $v=1$ levels of

the C state takes place after head formation, while complete predissociation takes place only after the $v=3$ level.²⁸ They have rotationally analyzed the (0,0) and (0,1) bands of this system recorded at a reciprocal dispersion of 0.22 Å/mm . They concluded that predissociation occurs at $J=73$ in the $v=0$ level of the $C^1\Pi$ state and attributed this predissociation to crossing of a $^1\Pi$ or a $^1\Delta$ state. The RKR potential curve for the C state and Franck–Condon factors for the $C-X$ transitions were also calculated. Wolf and Tiemann⁴⁰ reported on high resolution spectrum of the $C-X$ system of InCl excited by a frequency-doubled pulsed laser. They determined the potential energy curve for the $C^1\Pi$ state with three vibrational levels (e.g., $v'=0, 1, 2$) and found it to be a quasibound state with a shallow well. Wolf and Tiemann⁴⁰ observed discrete rotational structure in transition to the $v'=0$ level. The 1–0 band showed a sharp band head, but no resolvable rotational fine structure was seen. For transition involving $v'=2$, the linewidths were so large that the band head is strongly deformed. They concluded that an increase in the spectral linewidth with increasing vibrational quantum number is qualitatively in accordance with predissociation by tunneling. The rotational quantum numbers of the fine structure in the bands (0–0), (0–1), and (0–2), recorded at high resolution by laser tuning, for both isotopic combinations In³⁵Cl and In³⁷Cl, were assigned and effective parameters B_0 , D_0 , H_0 , etc. for the $C^1\Pi$ state were reported. Predissociation lifetime on the order of picoseconds was determined by an analysis of the linewidths. The potential curve of $C^1\Pi$ obtained by a nonlinear least-square procedure from the measured data shows a very shallow minimum at small internuclear distance and also a maximum is seen at an internuclear distance $r=2.74\text{ Å}$ which is responsible for the predissociation. Vibrational levels $v=0, 1, 2$, exist below the potential maximum. Vempati and McLean³⁵ recorded the $C-X$ system of InCl in absorption at a reciprocal dispersion 0.11 Å/mm and analyzed the rotational structure of six bands of the $(0,v')$ progression. They had observed a maximum J' value of 95, and determined the rotational constants for this C state of both isotopic molecules. Li *et al.*⁴⁹ measured the radiative lifetime for the $C^1\Pi$ state and calculated the electronic transition moment for the $B-X$ and $C-X$ systems of InCl. Most recently, Zou *et al.*⁵³ have performed a theoretical study of $C^1\Pi-X^1\Sigma^+$ transition of InCl using CCSD substitutions computations. The potential curve, spectroscopic constants, and the radiative lifetimes and tunneling predissociation lifetime for the different vibrational levels of $C^1\Pi$ state are computed. The calculated vibrational constants ω_e and $\omega_e x_e$ show only fair agreement, while the bound equilibrium distance r_e and the vertical excitation energy T_e are in good agreement with the corresponding experimental values. Zou *et al.*⁵³ concluded that the $C^1\Pi$ state is a quasibound state with a shallow well and the maximum vibrational quantum number for discrete levels in this state should not be more than 4 ($v'=0-3$) as reported by Perumalsamy *et al.*²⁸

4.2.3. InBr

For the InBr molecule bands attributed to the $C-X$ transition were first reported by Wehrli and Miescher,¹² in the region 286–311 nm. These authors assigned nine fluctuation bands as involving $v'=0$ and $v''=0-8$, though the separation between the successive bands (which would be a measure of the vibrational level spacing in the ground state) ranged from a high of 550 cm^{-1} to a low of 260 cm^{-1} . Even the lower value is much larger than the ω_e value of the X state. Later on Singh *et al.*³⁹ reported observation of diffuse bands of the $C-X$ system of InBr in absorption at different temperatures on a 1 m grating monochromometer. A partial potential energy curve for the $C^1\Pi$ state of InBr was also derived in this report³⁹ (Fig. 5). These authors reported that at the lowest temperature (300°C) only a broadband peak at 286.2 nm is observed, but as the temperature is increased the intensity of this peak gradually decreases and additional bands appear towards the longer wavelength side and finally merge in a continuum beginning at 311.0 nm. The largely diffuse character of the absorption bands and the onset of a continuum after the band convergence limit was explained by assuming that the upper state potential curve is very shallow (if it has any minimum). The observed nature of the fluctuation bands suggests that the left limb of the upper repulsive curve corresponds to r values nearly overlapping with the right turning ($r > r_e$) points in the lower (stable ground state) curve (Fig. 5).

4.2.4. InI

In InI the $C-X$ system was reported by Wehrli and Miescher¹² as a continuum with a maximum at 318.0 nm. No other report regarding this system in InI was found in the literature.

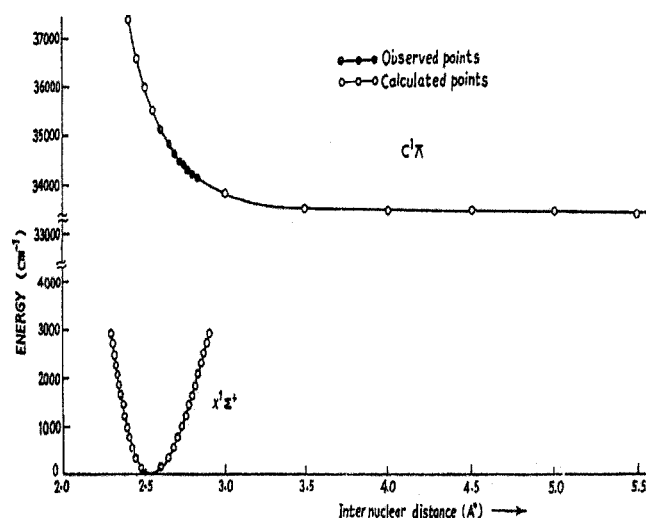


FIG. 5. Potential energy curve for the $X^1\Sigma^+$ and $C^1\Pi$ states of the InBr molecule.

4.3. The $D-X$ System

The $D-X$ system is reported only for the InF molecule in diatomic indium halides. This system for InF was observed by Barrow *et al.*^{14,15} The T_0 and ω_0 values for the D state of InF were reported as $47\,536$ and 535 cm^{-1} , respectively.

5. Rydberg States

5.1. InCl

Johnson *et al.*⁹ first reported 12 Rydberg states for the indium monochloride molecule using resonance enhanced multiphoton ionization (REMPI) spectroscopy thereby greatly extended the number of known electronic states. The REMPI spectra arise through one, two, and three photon resonance with excited states that lie between $27\,000$ and $75\,000\text{ cm}^{-1}$. Through extrapolation of the observed Rydberg series they have determined an adiabatic ionization potential (IP) (Table 1) that can support improved thermochemical calculations for InCl and InCl^+ . Table 7 summarizes the spectroscopic information derived for each Rydberg state, as reported by Johnson *et al.*⁹ The quantum defect of the Rydberg state is calculated using $\text{IP}=77\,460\text{ cm}^{-1}$.

Balfour and Chandrasekhar¹⁰² have reported an emission spectrum of InCl^+ and they carried out the rotational analysis for the $B^2\Sigma^+-X^2\Sigma^+$ system of this molecular ion. This system was earlier reported²³ as a band system of InCl but later on this was reassigned as belonging to InCl^+ . The above rotational analysis of the $B-X$ system of InCl^+ was found to be consistent with the photoelectron observations by Berkowitz and Dehmer.⁷⁴ A rough estimate of $X^2\Sigma^+$ state vibrational parameters for $\text{In}^{35}\text{Cl}^+$ are also obtained ($\omega_e''=354\text{ cm}^{-1}$ and $\omega_e''x_e''=4.9\text{ cm}^{-1}$).

Balfour and Chandrasekhar¹⁰² have suggested the following electron configurations for the relevant states:

$$\begin{aligned} \dots(z\sigma)^2(y\sigma)^2(\omega\pi)^4(x\sigma)^2: & \quad X^1\Sigma^+ \text{ InCl}, \\ \dots(z\sigma)^2(y\sigma)^2(\omega\pi)^4(x\sigma)^1: & \quad X^2\Sigma \text{ InCl}^+, \end{aligned}$$

TABLE 7. Summary of the spectroscopic information for the Rydberg states of InCl^a

State	λ_{origin} (nm)	REMPI mechanism	Principal quantum number	Quantum defect	$\Delta G_{1/2}$ (cm^{-1})	ν_{00} (obs) (cm^{-1})
F	365.14	2+1	6	3.801	355	54 757 ^b
G	360.40	2+1	6	3.766	333	55 478
H	349.11	2+1	6	3.669	332	57 259 ^b
I	480.89	3+1	6	3.303	338	62 371
J	478.71	3+1	6	3.278	318	62 650
K	459.14	3+1	7	3.993	335	65 321 ^b
L	449.47	3+1	7	3.802	...	66 726 ^b
M	447.86	3+1	7	3.766	...	66 966
N	444.17	3+1	7	3.676	325	67 527 ^b
Q	425.48	3+1	4	0.033	307	70 488
S	424.71	3+1	8	3.995	341	70 617 ^b
T	420.78	3+1	8	3.786	314	71 277 ^b

^aTaken from Johnson *et al.*⁹

^bValue is used for the calculation of IP_a .

$$\dots(z\sigma)^2(y\sigma)^2(\omega\pi)^3(x\sigma)^2: A^2\Pi \text{ InCl}^+,$$

$$\dots(z\sigma)^2(y\sigma)^1(\omega\pi)^4(x\sigma)^2: B^2\Sigma \text{ InCl}^+.$$

They have concluded from their study of the $B-X$ bands of InCl^+ that $(x\sigma)$ is antibonding while $(y\sigma)$ and $(\omega\pi)$ are bonding. The bonding in the X state in the ion is thus considerably stronger than in the corresponding neutral molecule. Glenewinkel-Meyer *et al.*⁸⁰ have reported on the electronic emission spectra of several group IIIA monohalide cations. They have also reported a $C^2\Pi$ and a $D^2\Sigma$ state in addition to the known $X^2\Sigma$, $A^2\Pi$, and $B^2\Sigma$, states for InCl^+ and InBr^+ .

5.2. InF, InBr, and InI

To the best of our knowledge, Rydberg states for these molecules are not known to date.

6. Laser Emission by Photodissociation of Indium Monohalides

Photodissociation of simple molecules has turned out to be a very effective pumping process for atomic resonance laser action in one of the photofragments.¹⁰³ Although the ground state of many metal-halide molecules are strongly bonded by ionic attraction, some of their excited states possess only weak covalent attraction and or are almost purely repulsive. As a result, excitation of these molecules by ultraviolet (UV) radiation often causes molecular dissociation



The product metal atom M^* can be in an excited atomic electronic state, with energy E_A , if $h\nu_{\text{pump}} > E_A + E_D$, where E_D is the dissociation energy of the ground molecular state.

UV photodissociation of alkali and group IIIA metal halides provides a simple method of producing metal-atom

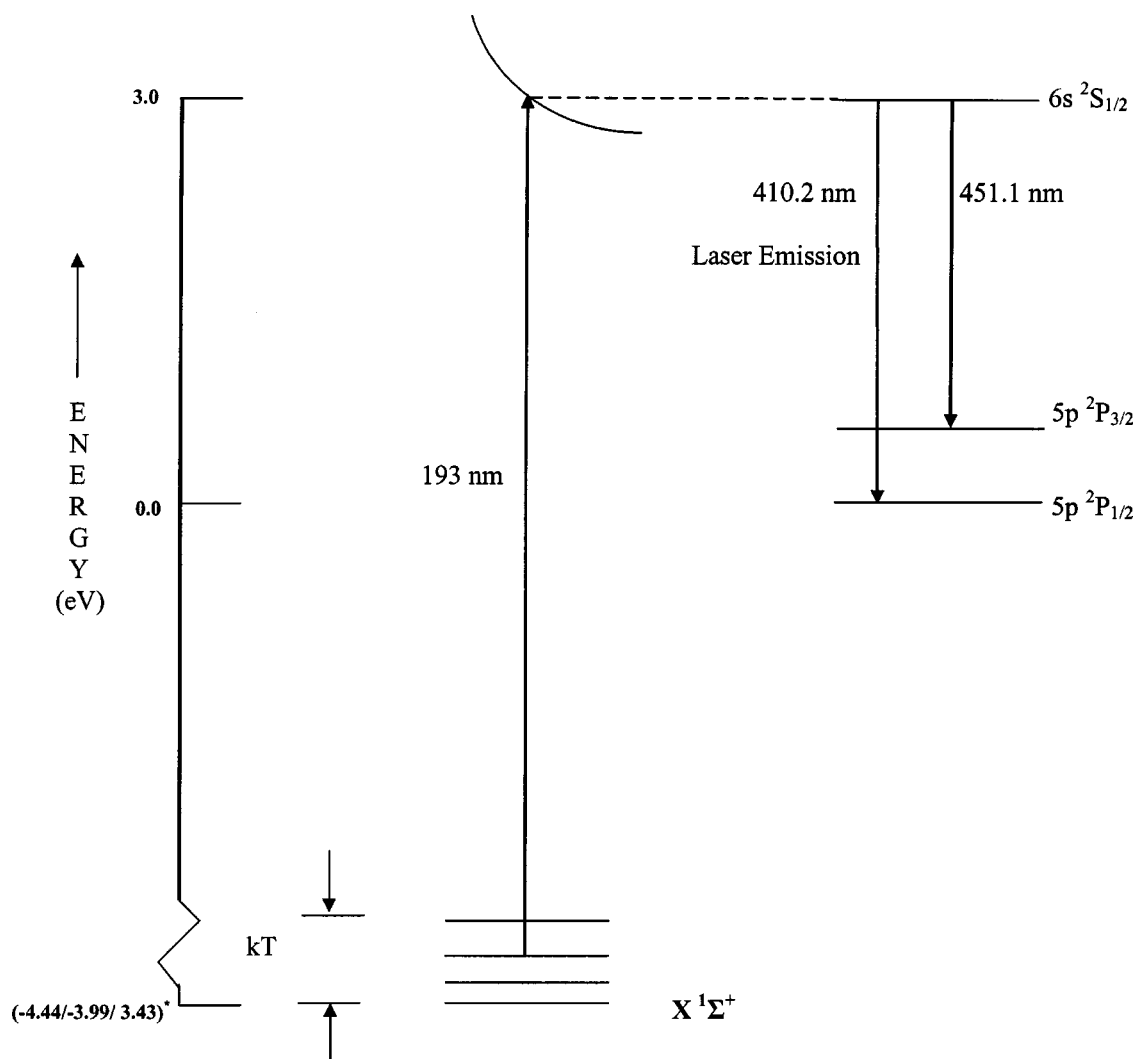


FIG. 6. Energy level diagram of indium halides and neutral indium relevant to indium photodissociation laser. The asterisk represents the corresponding values for InCl, InBr, and InI, respectively.

resonance line lasers.^{103,104} These lasers are useful for several applications involving long optical paths, such as in the remote sensing of the same metal atoms.¹⁰³ The lasers are potentially simple and inexpensive in construction. The threshold value for the UV pump energy is low, $\sim 10 \mu\text{J}$, and a variety of coherent or incoherent pump source can be used.¹⁰³ Metal-atom photodissociation lasers were first proposed by Zare and Herschbach¹⁰⁵ in 1965. Since then a number of studies have been carried out regarding such lasers.

It has been known that photodissociation of (diatomic) Tl halides by radiation of wavelength lower than 200 nm (e.g., 193 nm) leads to production of Tl atoms in the $7^2S_{1/2}$ state, which relaxes either by emitting 377 nm radiation, to the ground $6^2P_{1/2}$ state or, through emission of 535 nm radiation, to the metastable $6^2P_{3/2}$ state.² Therefore, it was not surprising that laser emission at these wavelengths should be expected and, in fact, was seen at both wavelengths in the case of TlI by Ehrlich *et al.*² and TlBr by Burkhard *et al.*⁵ and by Luthy *et al.*¹⁰⁶ The efficiency in the case of TlI was as large as 10%.

Burnham¹ obtained stimulated emission from indium ($6^2S_{1/2}-5^2P_{3/2}$ transition) at 451.1 nm in indium monoiodide vapor optically pumped by an ArF laser at 193 nm. The incident radiation causes dissociative excitation of the indium monoiodide leading to indium atom in the $6^2S_{1/2}$ (upper laser state) and an iodine atom in the $5^2P_{3/2}$ ground state (Fig. 6). Since no ground state In atoms are present, population inversion is obviously created and laser pulses with maximum energy of 0.5 mJ at 451 nm were obtained, from an absorption of 30 mJ of ArF laser radiation. Weak super-radiance was also observed on the 410.1 nm resonance line of indium. The output laser energy at 451 nm was observed to decrease gradually as the temperature of the cell was raised from 350 to 600 °C. The indium photodissociation laser appears to have the potential for efficient conversion of ultraviolet pump radiation to visible laser radiation.

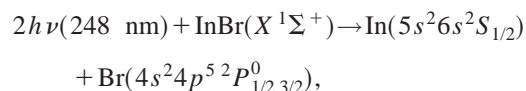
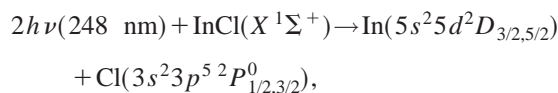
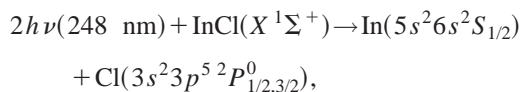
The fluorescence from indium atom attributable to two photon dissociative excitation in InCl and InBr using a 248 nm KrF laser source, has been reported by Cool and Koffend,⁷⁰ in continuation of their previous studies on mercury, lead and thallium halides.^{70,107}

The two photon-dissociative excitation process, i.e.,

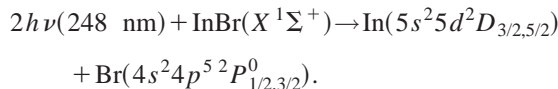


may also provide a useful means for the optical pumping of laser transition in many metal atoms, although until now laser action by this means has been observed only in Pb atoms.⁷⁰

Measurements of two-photon dissociative excitation cross sections are reported by Cool and Koffend⁷⁰ for the following processes:



and



The measured cross sections are seen to be much larger than those reported to date for two-photon transitions between bound molecular electronic states. The measurement of two photon absorption cross section for coupling between ground molecular states has been reported and compared with theory.¹⁰⁸

7. Conclusion

The four states— $X^1\Sigma^+$, $A^3\Pi_0^+$, $B^3\Pi_1$, and $C^1\Pi$ —are reasonably characterized for InF, InCl, InBr, and InI. However even for these states the potential energy curve is well understood only in the vicinity of the minima (only for energies less than 15%–20% of the dissociation energy). This leaves the question of the contribution of the ionic dissociation products completely unresolved. The ground state rotational constants are well determined from microwave studies but comparative results for the excited states need studies involving pure isotopic species. Another controversial point still needing more study is the question of predissociation in the $C^1\Pi$ state. The predissociating state is not well characterized. Information about Rydberg states are only available for InCl molecule and such studies are needed for other molecules of this group. Though some data on photodissociation cross sections are known, more detailed study is clearly needed to optimize the performance of the atomic indium laser. Recently, discrete Fourier transform calculations and other *ab initio* based calculations have been performed for the GaF, GaCl, GaBr, GaI, TlF, etc. Therefore, these calculations need to be extended to the indium monohalide molecule to confirm the nature of different excited electronic states.

8. Acknowledgments

The authors gratefully acknowledge the financial assistance provided by Dr. B. B. Singh, Principal, Udai Pratap Autonomous College, Varanasi. They are also grateful to Professor D. K. Rai, Department of Physics, Banaras Hindu University, Varanasi for valuable suggestions and discussions.

9. References

- ¹R. Burnham, Appl. Phys. Lett. **30**, 132 (1977).
- ²D. J. Ehrlich, J. Maya, and R. M. Osgood, Appl. Phys. Lett. **33**, 931 (1978).
- ³J. Maya, Appl. Phys. Lett. **32**, 484 (1978).

- ⁴H. Hemmati and G. J. Colline, *Appl. Phys. Lett.* **34**, 844 (1979).
- ⁵P. Burkhard, W. Luthy, and T. Gerber, *Opt. Commun.* **34**, 451 (1980).
- ⁶J. C. White and D. Henderson, *Phys. Rev.* **25**, 1226 (1982).
- ⁷J. L. Hastie, *High Temperature Vapors* (Academic, New York, 1975).
- ⁸J. F. Waymouth, *Electric Discharge Lamps* (MIT Press, Cambridge, MA, 1975).
- ⁹R. D. Johnson, D. V. Dearden, and J. W. Hudgens, *J. Chem. Phys.* **100**, 3422 (1994).
- ¹⁰M. Bruchhausen, J. Voigt, T. Doerk, S. Hadrich, and J. Uhlenbusch, *J. Mol. Spectrosc.* **201**, 70 (2000).
- ¹¹A. Petrikaln and J. Hochberg, *Z. Phys.* **86**, 214 (1933).
- ¹²M. Wehrli and E. Miescher, *Helv. Phys. Acta* **7**, 298 (1934).
- ¹³D. Welti and R. F. Barrow, *Proc. Phys. Soc. A* **65**, 629 (1952).
- ¹⁴R. F. Barrow, J. A. T. Jacquot, and E. W. Thompson, *Proc. Phys. Soc. A* **67**, 528 (1954).
- ¹⁵R. F. Barrow, D. V. Glazer, and P. B. Zeeman, *Proc. Phys. Soc. A* **68**, 962 (1955).
- ¹⁶H. M. Froslic and J. G. Winans, *Phys. Rev.* **72**, 481 (1947).
- ¹⁷P. Youngner and J. G. Winans, *J. Mol. Spectrosc.* **4**, 23 (1960).
- ¹⁸A. Lakshminarayana and P. B. V. Harnath, *Indian J. Phys.* **44**, 504 (1970).
- ¹⁹V. P. N. Nampoori, M. N. Kamalasanan, and M. M. Patel, *J. Phys. B: At. Mol. Phys.* **8**, 2841 (1975).
- ²⁰Ashrafunnisa, D. V. K. Rao, and P. T. Rao, *Spectrosc. Lett.* **9**, 9 (1976).
- ²¹M. L. P. Rao, D. V. K. Rao, and P. T. Rao, *Spectrosc. Lett.* **9**, 1976 (1976).
- ²²V. P. N. Nampoori and M. M. Patel, *Curr. Sci.* **45**, 369 (1976).
- ²³V. P. N. Nampoori and M. M. Patel, *Curr. Sci.* **48**, 532 (1979).
- ²⁴K. P. Huber and G. Herzberg, *Molecular Spectra and Molecular Structure, Constants of Diatomic Molecules* (Van Nostrand, Princeton, N.J., 1979), Vol. 4.
- ²⁵J. Borkowska-Burnecka and W. Zyrmicki, *Physica C* **115**, 415 (1983).
- ²⁶J. Borkowska-Burnecka and W. Zyrmicki, *Phys. Scr.* **35**, 141 (1987).
- ²⁷K. Perumalsamy, S. B. Rai, K. N. Upadhy, and D. K. Rai, *Physica C* **132**, 315 (1986).
- ²⁸K. Perumalsamy, S. B. Rai, and K. N. Upadhy, *Physica C* **141**, 315 (1986).
- ²⁹S. N. Vempati and W. E. Jones, *J. Mol. Spectrosc.* **119**, 405 (1986).
- ³⁰S. N. Vempati and W. E. Jones, *J. Mol. Spectrosc.* **120**, 441 (1986).
- ³¹S. N. Vempati and W. E. Jones, *Spectrosc. Lett.* **19**, 757 (1986).
- ³²S. N. Vempati and W. E. Jones, *J. Mol. Spectrosc.* **122**, 190 (1987).
- ³³S. N. Vempati and W. E. Jones, *J. Mol. Spectrosc.* **127**, 232 (1988).
- ³⁴S. N. Vempati and W. E. Jones, *J. Mol. Spectrosc.* **132**, 458 (1988).
- ³⁵S. N. Vempati and T. D. McLean, *J. Mol. Spectrosc.* **150**, 195 (1991).
- ³⁶V. B. Singh, A. K. Rai, S. B. Rai, and D. K. Rai, *Physica C* **144C**, 247 (1987).
- ³⁷V. B. Singh, A. K. Rai, S. B. Rai, and D. K. Rai, *J. Phys. B: At. Mol. Phys.* **20**, L45 (1987).
- ³⁸V. B. Singh, A. K. Rai, S. B. Rai, and D. K. Rai, *Indian J. Phys.* **62B**, 41 (1988).
- ³⁹V. B. Singh, S. B. Rai, and D. K. Rai, *J. Sci. Res. (B.H.U.)* **39**, 177 (1989).
- ⁴⁰U. Wolf and E. Tiemann, *Chem. Phys. Lett.* **139**, 191 (1987).
- ⁴¹E. Tiemann, *Mol. Phys.* **65**, 359 (1988).
- ⁴²S. P. Davis and R. Pecynner, *J. Opt. Soc. Am. B* **5**, 1995 (1988).
- ⁴³N. Badowski, *Spectrosc. Lett.* **21**, 589 (1988).
- ⁴⁴M. Singh, G. S. Ghodgaonkar, and M. D. Saksena, *J. Quantum Spectrosc. Radiat. Transfer* **46**, 583 (1991).
- ⁴⁵R. Venkatasubramanian, M. D. Saksena, and M. Singh, *Chem. Phys. Lett.* **210**, 367 (1993).
- ⁴⁶M. D. Saksena and M. N. Deo, *J. Mol. Spectrosc.* **208**, 64 (2001).
- ⁴⁷M. D. Saksena and M. N. Deo, *Ind. J. Phys.* **76B**, 503 (2002).
- ⁴⁸Y. Li, M. Lin, Q. Zhao, B. Zhang, W. Zou, and W. Chen, *Mol. Phys.* **97**, 607 (1999).
- ⁴⁹Y. Li, M. Lin, W. Zou, B. Zhang, and W. Chen, *Mol. Phys.* **98**, 1365 (2000).
- ⁵⁰K. Balasubramanian, J. X. Tao, and D. W. Liao, *J. Chem. Phys.* **95**, 4905 (1991).
- ⁵¹C. W. Bauschlicher, Jr., *J. Phys. Chem. A* **103**, 6429 (1999).
- ⁵²E. Lenthe and E. J. Baerends, *J. Chem. Phys.* **112**, 8279 (2000).
- ⁵³W. Zou, M. Lin, X. Yang, and B. Zhang, *Chem. Phys. Lett.* **356**, 523 (2002).
- ⁵⁴N. P. J. Vanstralen and L. Visscher, *J. Chem. Phys.* **117**, 3103 (2002).
- ⁵⁵A. H. Barrett and M. Mendel, *Phys. Rev.* **99**, 666 (1955).
- ⁵⁶A. H. Barrett and M. Mendel, *Phys. Rev.* **109**, 1572 (1958).
- ⁵⁷J. Hoeft, *Z. Phys.* **163**, 262 (1961).
- ⁵⁸G. A. L. Delvigne and H. W. De Wijn, *J. Chem. Phys.* **45**, 3318 (1966).
- ⁵⁹F. J. Iovas and T. Topping, *Z. Naturforsch.* **24a**, 634 (1969).
- ⁶⁰J. Hoeft, F. J. Lovas, E. Tiemann, and T. Topping, *Z. Naturforsch.* **25a**, 1029 (1970).
- ⁶¹B. Schenk, E. Tiemann, and J. Hoeft, *Z. Naturforsch.* **25a**, 1827 (1970).
- ⁶²E. Tiemann, J. Hoeft, and T. Topping, *Z. Naturforsch.* **27a**, 669 (1972).
- ⁶³R. H. Hammerle, R. V. Ausdal, and J. C. Zorn, *J. Chem. Phys.* **57**, 4068 (1972).
- ⁶⁴E. Tiemann, U. Kohler, and J. Hoeft, *Z. Naturforsch.* **32a**, 6 (1977).
- ⁶⁵H. Uehara, K. Horiai, T. Mitani, and H. Suguro, *Chem. Phys. Lett.* **162**, 137 (1989).
- ⁶⁶J. Hoeft and K. P. R. Nair, *Chem. Phys. Lett.* **155**, 273 (1989).
- ⁶⁷J. Hoeft and K. P. R. Nair, *Chem. Phys. Lett.* **164**, 33 (1989).
- ⁶⁸J. Hoeft and K. P. R. Nair, *Z. Phys. D* **29**, 203 (1993).
- ⁶⁹K. D. Hensel and M. C. L. Gerry, *J. Chem. Soc. Faraday Trans.* **93**, 1053 (1997).
- ⁷⁰T. A. Cool and J. B. Koffend, *J. Chem. Phys.* **74**, 2287 (1981).
- ⁷¹D. Cubicciotti, *J. Phys. Chem.* **60**, 1410 (1965).
- ⁷²H. Lefebvre-Brion and M. Moser, *J. Mol. Spectrosc.* **15**, 221 (1965).
- ⁷³J. Berkowitz, *J. Chem. Phys.* **56**, 2766 (1972).
- ⁷⁴J. Berkowitz and J. L. Dehmer, *J. Chem. Phys.* **57**, 3195 (1972).
- ⁷⁵J. Berkowitz and J. L. Dehmer, *J. Chem. Phys.* **58**, 568 (1973).
- ⁷⁶R. G. Egdell and A. F. Orchard, *J. Chem. Soc. Faraday Trans.* **274**, 1179 (1978).
- ⁷⁷G. Kim and K. Balasubramanian, *J. Mol. Spectrosc.* **152**, 192 (1992).
- ⁷⁸Y. Li, H. P. Liebermann, G. Hirsch, and R. J. Buenker, *J. Mol. Spectrosc.* **165**, 219 (1994).
- ⁷⁹O. Grabandt, C. A. De Lange, and R. Mooywan, *Chem. Phys. Lett.* **160**, 351 (1989).
- ⁸⁰Th. Glenewinkel-Meyer, A. Kowalski, B. Muller, and Ch. Ottinger, *J. Chem. Phys.* **89**, 7112 (1988).
- ⁸¹R. F. Barrow, A. C. P. Pugh, and F. J. Smith, *Trans. Faraday Soc.* **51**, 1657 (1955).
- ⁸²R. F. Barrow, *Trans. Faraday Soc.* **56**, 952 (1960).
- ⁸³E. M. Bulewicz, L. F. Phillips, and T. M. Sugden, *Trans. Faraday Soc.* **57**, 921 (1961).
- ⁸⁴E. Murad, D. L. Hildenbrand, and R. P. Main, *J. Chem. Phys.* **45**, 263 (1966).
- ⁸⁵Y. Ozaki, K. Horiai, K. Nukagawa, and H. Uehara, *J. Mol. Spectrosc.* **158**, 363 (1993).
- ⁸⁶U. Wolf and E. Tiemann, *Chem. Phys. Lett.* **119**, 407 (1988).
- ⁸⁷S. K. Mishra, R. K. S. Yadav, S. B. Rai, and V. B. Singh, *Indian J. Phys.* (accepted for publication).
- ⁸⁸G. Herzberg, *Spectra of Diatomic Molecules*, 2nd ed. (Van Nostrand, Princeton, N.J., 1950), p. 100.
- ⁸⁹N. B. Hannay and C. P. Smyth, *J. Am. Chem. Soc.* **68**, 171 (1946).
- ⁹⁰L. Pauling, *J. Phys. Chem.* **56**, 361 (1952).
- ⁹¹J. K. Wilmschurst, *J. Phys. Chem.* **30**, 561 (1959).
- ⁹²S. S. Batsanov and V. I. Durakov, *Struct. Chem.* **2**, 424 (1961).
- ⁹³S. N. Thakur, R. B. Singh, and D. K. Rai, *J. Sci. Res.* **27**, 339 (1968).
- ⁹⁴H. Hellmann, *Acta Phys. Chim. U.R.S.S.* **1**, 993 (1934).
- ⁹⁵E. S. Rittner, *J. Chem. Phys.* **19**, 1030 (1951).
- ⁹⁶H. Uehara, K. Horiai, T. Mitani, and H. Suguro, *Chem. Phys. Lett.* **162**, 137 (1989).
- ⁹⁷K. P. R. Nair and J. Hoeft, *J. Mol. Spectrosc.* **85**, 301 (1981).
- ⁹⁸W. J. Balfour, K. S. Chandrasekhar, and M. D. Saksena, *J. Mol. Spectrosc.* **145**, 458 (1991).
- ⁹⁹W. Grotrian, *Z. Phys.* **11-12**, 218 (1922).
- ¹⁰⁰E. Miescher and M. Wehrli, *Helv. Phys. Acta.* **6**, 256 (1933).
- ¹⁰¹H. Haragachi and K. Fuwa, *Spectrochim. Acta B* **30**, 535 (1975).
- ¹⁰²W. J. Balfour and K. S. Chandrasekhar, *J. Mol. Spectrosc.* **124**, 443 (1987).
- ¹⁰³D. J. Ehrlich and R. M. Osgood, Jr., *IEEE J. Quantum Electron.* **QE-16**, 257 (1980).
- ¹⁰⁴J. Maya, *IEEE J. Quantum Electron.* **QE-15**, 579 (1979).
- ¹⁰⁵R. N. Zare and D. R. Herschbach, *Appl. Opt.* **2**, 193 (1965).
- ¹⁰⁶W. Luthy, P. Burkhard, T. E. Gerber, and H. P. Weber, *Opt. Commun.* **38**, 413 (1981).
- ¹⁰⁷T. A. Cool, J. A. McGraevy, Jr., and A. C. Erlandson, *Chem. Phys. Lett.* **58**, 108 (1978).
- ¹⁰⁸D. J. Kligler and C. K. Rhodes, *Phys. Rev. Lett.* **40**, 309 (1978).